INSTITUTE OF PHYSICS PUBLISHING NONLINEARITY

Nonlinearity **18** (2005) R17–R44 doi:10.1088/0951-7715/18/6/R01

INVITED ARTICLE

Recent progress in understanding the transition to turbulence in a pipe

R R Kerswell

Department of Mathematics, University of Bristol, UK

E-mail: R.R.Kerswell@bris.ac.uk

Received 29 March 2004, in final form 23 June 2005
Published 8 August 2005
Online at stacks.iop.org/Non/18/R17

Recommended by C P Dettmann

Abstract

The problem of understanding the nature of fluid flow through a circular straight pipe remains one of the oldest problems in fluid mechanics. So far no explanation has been substantiated to rationalize the transition process by which the steady unidirectional laminar flow state gives way to a temporally and spatially disordered three-dimensional (turbulent) solution as the flow rate increases. Recently, new travelling wave solutions have been discovered which are saddle points in phase space. These plausibly represent the lowest level in a hierarchy of spatio-temporal periodic flow solutions which may be used to construct a cycle expansion theory of turbulent pipe flows. We summarize this success against the backdrop of past work and discuss its implications for future research.

PACS numbers: 47.27.Cn, 47.20.Ft

(Some figures in this article are in colour only in the electronic version)

1. Introduction

Ever since the pioneering experimental work of Osborne Reynolds (1883), the issue of how and why the fluid flow along a circular pipe changes from being laminar (highly ordered in space and time) to turbulent (highly disordered in both space and time) as the flow rate increases has intrigued physicists, mathematicians and engineers alike. The problem, of course, is not that we do not know the governing equations of motion since we do—they are the celebrated Navier–Stokes equations. Rather the challenge is to extract the relevant information from this notoriously difficult set of nonlinear equations to rationalize what we see. One promising idea emerging from dynamical systems theory is to use unstable periodic solutions as building blocks in a weighted expansion to describe temporally and spatially

 © 2005 IOP Publishing Ltd and London Mathematical Society Printed in the UK

complicated flows (Cvitanović 1988, Artuso *et al* 1990a, 1990b). This has been successfully applied in low-dimensional dynamical systems and quantum mechanics (e.g. Artuso *et al* (1990b) and references herein, Cvitanović (1992) and later papers in the same journal issue, Cvitanović *et al* (2005)) as well as a one-space-and-time partial differential equation (PDE) setting (the Kuramoto–Shivashinsky equation: Christiansen *et al* (1997)) but remains untested for a fully 3-spatial dimension nonlinear PDE system like the Navier–Stokes equations. The primary reason for this is the difficulty in initially finding all the dynamically important unstable periodic orbits—perhaps more accurately described as recurring spatio-temporal patterns—in such a high-dimensional setting. Recently, however, the first successes have been made in this direction for pipe flow by the discovery of travelling wave solutions (Faisst and Eckhardt 2003, Wedin and Kerswell 2004). These periodic solutions are actually stationary states when viewed from a frame translating with a constant phase speed (which depends on the wave structure) down the pipe and therefore represent the lowest rung in the hierarchy of phase space structures which could potentially be used to characterize mean properties of the flow either in the transitional or fully turbulent regime. They are found to exist down to flow rates significantly below those at which transition is observed to occur. This seems to indicate that transition to turbulence is delayed until the stable and unstable manifolds of these saddle points become sufficiently tangled with each other (with increasing flow rate) to sustain complicated time-dependent flow trajectories away from the laminar fixed point in phase space.

The purpose of this paper is to describe how these travelling wave states were found as numerical solutions to the governing Navier–Stokes equations, to put their discovery in historical perspective and to discuss their implications for future work.

For many fluid dynamicists, pipe flow remains *the* classical problem of stability theory not only because of its historical pedigree but because the gap between theory and experiment has remained perhaps the largest across all the canonical flow stability problems that have been studied subsequently. The reasons for this are multifold. First, and most important, all experimental and theoretical evidence points to the fact that the laminar flow state (which exists for all flow rates) is linearly stable to any infinitesimal disturbance. The clear implication is that the observed transition process can then only be initiated by finite amplitude disturbances. Mathematically, this means that the laminar solution does not offer a bifurcation point at some finite flow rate which could be used as a starting point to generate new alternative (preferred) solutions to the governing equations as in the cases of Rayleigh–Bénard convection, Taylor–Couette flow or plane Poiseuille flow. In these flows, an ordered sequence of bifurcations can be traced in which the preferred flow becomes progressively more complicated in space and time. In contrast, the transition in pipe flow is rather delicate but when triggered leads abruptly to a complicated, disordered state. This absence of an initial bifurcation from the laminar state has meant that theoretical work has largely had to concentrate upon direct numerical simulation (DNS) as its tool of enquiry with limited tangible results.

Second, many experimental studies over the years have highlighted the somewhat surprising, spatially intermittent behaviour of transitional pipe flow—disordered motion arises in patches separated by regions of laminar flow—for a range of flow rates beyond that required to sustain turbulence. As a result pipe flow *has* become the canonical example of this phenomenon. The detailed data collected by probing these disordered patches has also served to emphasize the lack of any accompanying theoretical understanding beyond post rationalization through DNS.

Third, the fact that a pipe is cylindrical rather than planar and that transition occurs at higher relative flow rates than in other canonical planar shear flow such as the closely associated plane Couette flow or plane Poiseuille flow, has meant that it is less theoretically

accessible than these alternatives. As a result, pipe flow has been the least studied using analytical and numerical techniques although being most easily realized in the laboratory. The recent theoretical discovery of travelling wave solutions in pipe flow (Faisst and Eckhardt 2003, Wedin and Kerswell 2004) and their apparent observation soon after in experiments (Hof *et al* (2004): see also the commentaries Barenghi (2004), Busse (2004)) has however helped redress this imbalance. These solutions provide the first solid theoretical stepping stones beyond the laminar basic state from which to explore the transitional dynamics of pipe flow.

The plan of this paper is as follows. In section 2, the governing Navier–Stokes equations are written down along with some parameter definitions for the core problem of understanding the transition to turbulence in an incompressible Newtonian fluid flowing along a smooth, cylindrical straight pipe. Section 3 reviews past achievements in understanding the pipe flow problem with an emphasis on the theoretical side because a detailed review of experimental work is being prepared elsewhere (Mullin 2005). Section 4 details how the travelling waves were found numerically, describes their flow structure and indicates where they are to be found in parameter space. Section 5 discusses the significance of the travelling waves from a dynamical systems perspective before a final section 6 considers the exciting outlook for future research.

2. Notation

Here we set up notation for the rest of the paper. For an incompressible fluid of constant density ρ and kinematic viscosity ν flowing in a circular pipe of radius s_0 under the action of a constant applied pressure gradient

$$\boldsymbol{\nabla} p^* = -\frac{4\rho\nu W}{s_0^2}\hat{\boldsymbol{z}} \tag{2.1}$$

(where $\hat{\boldsymbol{z}}$ is directed along the pipe axis), the realized flow is known to be for long times uniquely of the parabolic form

$$\boldsymbol{u}^* = W\left(1 - \frac{s^2}{s_0^2}\right)\hat{\boldsymbol{z}} \tag{2.2}$$

at low enough values of the Reynolds number

$$Re := \frac{s_0 W}{\nu}, \tag{2.3}$$

where s is the radius in the normal cylindrical coordinates (s, ϕ, z). The governing Navier–Stokes equations (non-dimensionalized using the centreline speed W of the parabolic laminar flow and pipe radius s_0) for pipe flow are

$$\boldsymbol{u}_t + \boldsymbol{u}\cdot\boldsymbol{\nabla}\boldsymbol{u} + \boldsymbol{\nabla} p = \frac{1}{Re}\nabla^2\boldsymbol{u} + \frac{4}{Re}\hat{\boldsymbol{z}}, \tag{2.4}$$

$$\boldsymbol{\nabla}\cdot\boldsymbol{u} = 0, \tag{2.5}$$

with non-slip velocity boundary condition

$$\boldsymbol{u}(1, \phi, z) = \boldsymbol{0}, \tag{2.6}$$

where $\boldsymbol{u} = \boldsymbol{u}^*/W$ and p represents the pressure deviation away from the imposed gradient. State-of-the-art pipe flow experiments aim to ensure constant mass flux along the pipe as

opposed to constant pressure gradient either by sucking the fluid through (Hof *et al* 2003) or by pumping the flow with feedback to maintain an approximately constant flux (Draad *et al* 1998)—see Mullin (2005) for a detailed discussion. In this case it makes more sense to work with a 'mass-flux' Reynolds number

$$Re_m := \frac{2s_0\overline{W}}{\nu} \tag{2.7}$$

based upon the mean flow

$$\overline{W} := \frac{1}{\pi}\int_0^{2\pi} \mathrm{d}\phi \int_0^1 s\,\mathrm{d}s\,\boldsymbol{u}^*\cdot\hat{\boldsymbol{z}} \tag{2.8}$$

along the pipe. The ratio

$$\frac{Re_m}{Re} = \frac{2\overline{W}}{W} \leqslant 1 \tag{2.9}$$

is a measure of the mass flux relative to that of the laminar solution and indicates how 'far' the solution is away from the laminar state $\boldsymbol{u} = (1-s^2)\hat{\boldsymbol{z}}$ where the ratio is maximally one.

3. Background

3.1. Experimental work

Characterizing the resistance felt by a fluid when flowing through a circular pipe has been a fundamental problem in fluid mechanics since the beginning of the subject. Although the earliest traceable study is perhaps the treatise of Mariotte (1686), the first serious experimental studies are generally considered to be those carried out independently by the German engineer Gotthilf Hagen (1839) and the French physician Jean Poiseuille (1840) (see Rouse and Ince (1957)). Poiseuille studied the resistance in small capillaries (diameters ranging from 0.015 to 0.6 mm: see Sutera and Skalak (1993)) and thereby concentrated unwittingly on the steady unidirectional laminar flow invariably realized. Hagen, in contrast, used much larger diameters (2.5–6 mm) and noticed that another type of flow in which the motion was unsteady and three-dimensional could be realized beyond the steady laminar response (2.2) now known as the Hagen–Poiseuille flow (HPF). He worked on characterizing the resistance laws for both types of motion but never reached the point of isolating a general similarity parameter involving the fluid viscosity to describe his findings. This was to be Osborne Reynolds' triumph in his now famous 1883 study of the transition of the laminar Hagen–Poiseuille solution to 'sinuous' flow consisting of unsteady eddies.

Reynolds realized that a non-dimensional number corresponding to the ratio of dissipative D^2/ν to advective $D/\overline{W}$ times was sufficient to characterize the onset of eddy motion (where D is the diameter of the pipe, $\overline{W}$ is the mean flow along the pipe and ν is the kinematic viscosity of the fluid). The fact that many shear flows depend only on this 'Reynolds' number, Re_m, is one of the first things taught in any fluid dynamics course. Surprisingly, however, Reynolds failed to realize that his new parameter may also completely characterize the flow resistance function: Blasius demonstrated this later for smooth pipes (Blasius 1913). Characterizing the form of the flow resistance and mean velocity field as a function of Re_m has continued to attract attention (e.g. Prandtl (1927), Nikuradse (1932), Zagarola and Smits (1998), Swanson *et al* (2002), McKeon *et al* (2004a, 2004b)).

Reynolds' other great discovery in 1883 was the fact that the transitional Reynolds number Re_m^{t} varied with the level of disturbance in the flow. He found $Re_m^{\mathrm{t}} \approx 2000$ in

one series of experiments whereas in a more tightly controlled environment, transition was delayed until ≈12 000. Subsequent experimental work has essentially confirmed Reynolds' lowest critical value with current estimates varying across the range $1760 < Re_m^t < 2300$ (Binnie and Fowler 1947, Lindgren 1958, Leite 1959, Wygnanski and Champagne 1973, Darbyshire and Mullin 1995). In contrast, Reynolds' upper value has now been raised to 100 000 by suppressing the level of ambient disturbances even further (Pfenniger 1961). The clear implication of all this work is that there exists a finite-amplitude disturbance threshold to trigger transition and that this threshold decreases as Re_m increases.

Reynolds also found that when the flow became disordered it did so in patches separated by laminar regions. This spatial intermittency was examined more carefully by Wygnanski and co-workers in the 1970s who found what they thought were two different turbulent states christened 'puffs' and 'slugs' (Wygnanski and Champagne 1973, Wygnanski *et al* 1975). A puff was identified as a turbulent region with a sharp upstream boundary but whose downstream border is blurred due to the presence of larger-scale structures centred at the pipe axis which gradually peter out. Found for $2000 < Re_m < 2700$ and typically of 20–30 pipe diameters in length, the speeds of the upstream and downstream fronts are roughly equal and just less than the mean flow so that, on average, fluid passes through the puff on its way downstream. Puffs were generated by introducing large disturbances in the pipe inlet and viewed as an 'incomplete relaminarization process'.

A turbulent slug on the other hand was found to have two well defined fronts upstream and downstream enclosing turbulence which extended across the whole pipe cross section and which looked indistinguishable from fully turbulent pipe flow. Found to exist for $Re_m > 3200$, the upstream front moves slower than the mean flow speed whereas the downstream front moves faster so that the slug grows in spatial extent as it is advected down the pipe and fluid entrained into the slug never relaminarizes. Wygnanski's group considered only the slugs to be associated with the transition from laminar to turbulent flow, believing them to be the end product of a boundary layer instability in the pipe inlet region.

At this point, all experimental work had either relied on an imposed disturbance in the inlet flow (e.g. Wygnanski and Champagne (1973)) or a permanent but spatially localized perturbation in the fully developed flow to trigger transition (e.g. Fox *et al* (1968)). To avoid studying the wrong process (inlet instability or instability of *perturbed* HPF), attention was then focused on applying a spatially *and* temporally-localized (impulsive) disturbance to fully-developed HPF. Importantly, Rubin *et al* (1980) found that the structure of the transitional flow remains the same as that produced by a disturbed inlet provided the disturbance amplitude is large enough. The observed transitional behaviour also remains qualitatively similar if the flow is driven under constant-mass-flux conditions rather than the original pressure-driven system of Reynolds (Darbyshire and Mullin 1995). Darbyshire and Mullin, however, did fail to find the clear separation described by Wygnanski and Champagne (1973, figure 2b) in disturbance amplitude and Re_m for puffs and slugs to exist. They found both can exist over a range of Re_m depending on the type and not just the size of disturbance used. Using an impulsive perturbation, they also mapped out the finite amplitude stability curve (where 'amplitude' is defined as the ratio of the perturbation mass injection rate to the total mass flux) such that disturbances with amplitudes greater than the threshold produce transition while smaller ones decay downstream. It soon became clear that the amplitude threshold is also very sensitive to the frequency of the perturbation (Draad *et al* 1998) as well as to its azimuthal structure (Eliahou *et al* 1998, Han *et al* 2000). Recent work by Hof *et al* (2003, summarized in the popular article by Fitzgerald (2004)) has found that the threshold amplitude curve can be lowered to one scaling like Re_m^{-1} over the range $2000 < Re_m < 20\,000$ provided the perturbation is applied for long enough.

3.2. Theoretical work

The initial theoretical response to Reynolds' experiments was to examine the plight of small perturbations to HPF. Rayleigh (1892) found that inviscid, infinitesimal disturbances do not grow on laminar pipe flow, that is, HPF is inviscidly, linearly stable (see also the discussion by Kelvin (1887a, b)). Sexl (1927) incorporated the effects of viscosity but found HPF still linearly stable to axisymmetric disturbances at high Re (later proved by Herron (1991)). Subsequently there have been many theoretical (e.g. Gill (1965, 1973), Davey and Drazin (1969)) and numerical studies (Lessen *et al* 1968, Garg and Rouleau 1972, Salwen and Grosch 1972, Salwen *et al* 1980, Meseguer and Trefethen 2003) concentrating on the stability to asymmetric disturbances. The consensus now is that the flow is linearly stable to these too although a formal proof remains elusive.

At the other end of the theoretical spectrum, Joseph and Carmi (1969) established that a disturbance to HPF of *any* amplitude would exponentially decay—i.e. HPF is a global attractor—provided $Re < 81.49$. Interestingly, the first disturbance able to extract energy out of HPF (as Re is increased to 81.49) is unusually streamwise-dependent (helical) with azimuthal and streamwise wavenumbers of precisely and about one respectively. The large gap in Re between this energy stability value of 81.49 and the lowest transitional value of $\approx$2000, however, served only to emphasize the gulf between experiment and theory at that time. It was soon realized that this gap could be closed by rotating the pipe about its axis quickly but this is then a very different problem (Mackrodt (1976): rotating HPF becomes linearly unstable at a Re which approaches 82.88 from above as the rotation rate $\rightarrow \infty$ with 81.49 still being the energy stability limit).

Given the mounting evidence that HPF is linearly stable, efforts switched to constructing weakly nonlinear states around the least decaying linear disturbances. Davey and Nguyen (1971) and Itoh (1977) independently developed finite amplitude expansions for axisymmetric disturbances supposedly valid in the limit of $Re \rightarrow \infty$. Differing in only the ordering of terms, their results unfortunately contradicted each other indicating a lack of convergence of the series (Davey 1978). However, Gill realized that simple dimensional analysis arguments were able to reproduce the gross scaling results of Davey and Nguyen (1971, see appendix). The underlying premise for such an approach is that *if* a finite amplitude solution is wholely concentrated at the wall or at the pipe centre, the only relevant length scale would be set by the local HPF shear (at the wall) or curvature (at the axis). Numerical calculations by Patera and Orszag (1981), however, failed to find any axisymmetric equilibria. In a follow-up paper, Orszag and Patera (1983) found evidence that pipe flow is susceptible to a strong non-axisymmetric secondary instability of decaying axisymmetric states.

At about this time, Smith and Bodonyi (1982) applied the nonlinear critical layer theory of Benney and Bergeron (1969) to pipe flow at asymptotically large Re. They found neutral, finite-amplitude disturbances but only with an azimuthal wavenumber one structure of $O(Re^{-1/3})$ (rising to $O(Re^{-1/6})$ in the critical layer) coupled with $O(Re^{-1/6})$ mean axial and azimuthal (swirl) flow. Subsequently, Walton (2002) has shown how these disturbances can be reached as endstates of linear instabilities to impulsively started pipe flow. However, numerical computations by Landman (1990) for Re up to 4000 failed to find any evidence of these states.

Around the early nineties, attention refocused upon the ability of certain disturbances to undergo temporary algebraic growth in shear flows (Boberg and Brosa (1988), Gustavsson (1991), Butler and Farrell (1993), Reddy and Henningson (1993), Trefethen *et al* (1993); see also Tumin (1996) and Reshotko and Tumin (1999) for a spatial version of the theory) following the initial works by, for example, Case (1960), Benney (1961, 1964) and Stuart (1965).

Physically, the mechanism is simply one by which a small initial disturbance with some wall-normal velocity advects the large mean shear either away from or towards the wall. Typically, these wall-normal velocities only experience weak viscous decay and so their slow but sustained advection of the mean shear can produce large local anomalies in the streamwise velocity called streaks. Mathematically, this 'transient growth' is caused by the apparently generic non-normality of the linear operator governing the temporal evolution of infinitesimal disturbances in shear flows. This non-normality means that the eigenfunctions of the linear operator are not orthogonal (under the energy norm) with the consequence that certain initial flow conditions are poorly spanned. This ill-conditioning means that the eigenfunction expansion for some certain initial conditions requires unusually large coefficients due to a subset of eigenfunctions significantly cancelling. When each eigenfunction decays exponentially over time (otherwise the flow would be linearly unstable) they do so with different rates so that the initial cancellation melts away. This uncovers the large coefficients in the expansion which has the effect of producing a period of algebraic growth. A simple example from the appendix of Schmid and Henningson (1994) illustrates the point nicely (see also Eckhardt and Pandit (2003)). Consider the two-dimensional linear evolution equation

$$\frac{\mathrm{d}}{\mathrm{d}t}\begin{bmatrix} x \\ y \end{bmatrix} = \mathrm{A}\begin{bmatrix} x \\ y \end{bmatrix} := \begin{bmatrix} \dfrac{-1}{Re} & 0 \\ 1 & \dfrac{-2}{Re} \end{bmatrix}\begin{bmatrix} x \\ y \end{bmatrix}, \tag{3.10}$$

where Re is a model Reynolds number (i.e. a large parameter) and A is a non-normal matrix, i.e. A does not commute with its adjoint ($\mathrm{A}^{\mathrm{T}}\mathrm{A} \neq \mathrm{A}\mathrm{A}^{\mathrm{T}}$). The eigenvalues of A, $-1/Re$ and $-2/Re$, are both negative and therefore any initial condition in $\mathcal{R}^2$ is assured to asymptotically decay to zero as $t \to \infty$. However the associated eigenvectors

$$\frac{1}{\sqrt{1+Re^2}}\begin{bmatrix} 1 \\ Re \end{bmatrix} \qquad \text{and} \qquad \begin{bmatrix} 0 \\ 1 \end{bmatrix} \tag{3.11}$$

are not orthogonal and poorly span the x direction. Hence an initial condition $(x, y) = (1, 0)$ experiences initial algebraic growth before ultimately decaying

$$\begin{bmatrix} x(t) \\ y(t) \end{bmatrix} = \begin{bmatrix} 1 \\ Re \end{bmatrix}\mathrm{e}^{-t/Re} - \begin{bmatrix} 0 \\ Re \end{bmatrix}\mathrm{e}^{-2t/Re} \approx \begin{bmatrix} 1 - \dfrac{t}{Re} + O\left(\dfrac{t}{Re}\right)^2 \\ t + O\left(\dfrac{t}{Re}\right)^2 \end{bmatrix}. \tag{3.12}$$

The algebraic growth persists until $t = O(Re)$ and thus amounts to an $O(Re)$ amplitude growth. It is equally important to notice that this growth is not modal in the sense that the initial condition is simply magnified in amplitude. Rather the initial condition is rotated and amplified in another direction. Work in pipe flow (Boberg and Brosa 1988, Bergström 1992, 1993, O'Sullivan and Breuer 1994a, Schmid and Henningson 1994) has revealed that the initial perturbation which experiences the largest growth takes the form of two-dimensional streamwise-independent vortices (rolls) with a unity azimuthal wavenumber (equivalent to the initial condition $(x, y) = (1, 0)$ in the above example). Since such streamwise rolls have viscous decay rates of $O(Re^{-1})$ they can persist over an $O(Re)$ timescale with no energy source. During this period streamwise rolls of amplitude $O(\epsilon)$ can advect fluid across the $O(1)$ mean shear a distance $O(\epsilon Re)$ and thereby produce $O(\min(\epsilon Re, 1))$ 'streaks' or azimuthal (spanwise) variations in the mean flow (equivalent to $(x, y) = (0, 1)$ in the above example). In this linearized picture, an initial disturbance in the form of streamwise rolls can be amplified by a factor of $O(Re^2)$ in *energy* (changing structure into streaks) before ultimately decaying over an $O(Re)$ time.

Given this apparently potent linear amplification process, thinking naturally turned to examining how energy could be fed back from the streaks into the secularly-decaying rolls so that the process could be sustainable and thereby accomplish transition. Simple models invoking generic mixing by the nonlinearity of the Navier–Stokes equations (e.g. see Baggett and Trefethen (1997), Gebhardt and Grossman (1994)) proved successful but an oversimplification of the situation (Waleffe (1995a): see Benney and Gustavsson (1981), Boberg and Brosa (1988), Brosa and Grossmann (1999) for more serious attempts to understand the nonlinear feedback processes, as well as the review by Grossmann (2000)). Streamwise-independent perturbations which experience the largest transient growth cannot be self-sustaining according to the Navier–Stokes equations. Moreover their nonlinear development adjusts the mean flow in such a way as to reduce the transient growth possible. Clearly further flow structures needed to be excited and the obvious candidate process was the instability of finite-amplitude streaks. With this in mind, Zikanov (1996) studied the three-dimensional linear instability of pipe flow with two-dimensional streamwise rolls initially added. He found that once the rolls induce large enough spanwise modulation of the streamwise velocity (i.e. streaks), inflection points appear which are highly (inertially) unstable to three-dimensional disturbances. This approach mimicked the original work of Orszag and Patera (1983) which probed for secondary instability but by choosing an axially-invariant rather than an axisymmetric two-dimensional modulation (or primary flow), Zikanov found far larger potential for growth. In other words, the transient growth of the initial modulation to produce unstable streak structures meant that the starting amplitude needed to trigger secondary instability was necessarily smaller.

At about this time, interest was shifting from the traditional question of how turbulence is initiated to answering the question of how turbulence *maintains* itself. Jiménez and Moin (1991) pioneered the idea of a 'minimal' channel flow unit in which the spanwise and streamwise dimensions are reduced to the least values needed to sustain turbulence in DNS. Using this approach in plane Couette flow, Hamilton *et al* (1995) managed to identify a spatially and temporally organized cycle of events appearing to underpin the turbulence (following speculation of just such in Waleffe *et al* (1993)). This consisted of three phases: formation of streaks by streamwise vortices, breakdown of the streaks and the regeneration of the streamwise vortices. The last process was least understood being fundamentally nonlinear but it appeared that the streak instability directly regenerated the streamwise vortices through its nonlinear self-interaction. Waleffe (1995b, 1997) theoretically explored this observation by cutting open the Navier–Stokes equations and confirming the feasibility of each phase in isolation. Most importantly, he was able to demonstrate that a streak instability could indeed directly feed energy back into the streamwise rolls hence potentially establishing a self-sustained process (SSP); see Waleffe (1997) for low-dimensional models and Dauchot and Vioujard (2000) and Moehlis *et al* (2004, 2005) for phase space explorations. Significantly, Waleffe (1998, 2001, 2003) was able to convert this piecemeal verification analysis into a smooth numerical continuation procedure which has generated nonlinear steady state solutions and travelling wave solutions in plane Couette and travelling wave solutions in plane Poiseuille flows to arbitrary accuracy. These states consist of the three flow structures—streamwise vortices (rolls), streaks and waves (streak instabilities) blended together in such a way that they maintain each other symbiotically against viscous decay. The thinking was that one of these solutions—christened exact coherent structures (ECS) by Waleffe—acted as an organizing centre for the turbulence quasi-cycle found by Hamilton *et al* (1995). Kawahara and Kida (2001) have confirmed that a periodic orbit does exist there consisting of a time-dependent version of Waleffe's SSP.

Following Hamilton *et al* (1995) and Zikanov (1996), Reddy *et al* (1998) studied streak instability in plane Couette and Poiseuille flow establishing the generic nature of the process.

The appearance of this secondary instability was considered enough to signify turbulent transition. Numerical computations in pipe flow by Ma *et al* (1999) further confirmed this evolutionary sequence of rolls → streaks → streak instability → turbulence.

Other DNS work has been directed at probing the 'puffs' and 'slugs' structures produced in transitional flows (Leonard and Reynolds 1985, Nikitin 1994, O'Sullivan and Breuer 1994b, Shan *et al* 1999, Priymak and Miyazaki 1998, 2004, Reuter and Rempfer 2004). The general conclusion is that achievable numerical solutions of the Navier–Stokes equations are starting to reproduce at least qualitatively what is seen and measured in experiments. The major difficulty is ensuring the computational pipe is long enough (while maintaining cross sectional resolution) so that transitional structures can evolve without being influenced by artificial numerical boundary conditions. This is an ongoing challenge in the transitional regime but is not an issue for fully developed turbulent flow where correlation lengths are small. For example, Eggels *et al* (1994) find favourable quantitative comparison between fully developed turbulent flow seen experimentally at $Re_m \approx 5300$ and numerical results from a short (periodic) pipe of length 5 diameters at the same Re_m. Recently, Gavarini *et al* (2004) have returned to the issue of pipe inlet conditions by examining the effect of imposing very small but persistent axisymmetric (and axially invariant) distortions to HPF. Suitably chosen, these can make the base flow linearly unstable and transition occurs more readily. They discuss two scenarios: amplification of axisymmetric disturbances and the growth and breakdown of streaks. Significantly, the latter streak breakdown process is found to be the more robust mechanism under reduction of the length of the pipe over which the base distortion is imposed.

4. Travelling waves in pipe flow

Waleffe's success in developing a mechanistically motivated continuation procedure to generate nonlinear ECS solutions was particularly significant for the pipe flow problem. Homotopy—the approach by which known nonlinear solutions in a neighbouring problem are smoothly continued back to the original system of interest—had already been exploited with considerable success in other problems. Most notably in 1990, Nagata discovered the first nonlinear steady states in plane Couette flow using homotopy from rotating plane Couette flow. Further successes followed by building solution 'bridges' between Benard convection, Taylor–Couette flow and plane Couette flow (Nagata 1990, 1997, 1998, Clever and Busse 1992, 1997, Faisst and Eckhardt 2000). However, no continuation strategy back to pipe flow from another physical system had thus far succeeded. Efforts to repeat Nagata's success by trying to continue solutions known in rotating pipe flow (Toplosky and Akylas 1988) back to non-rotating pipe flow failed (Barnes and Kerswell 2000), and an attempt to use a geometrical embedding of (circular) pipe flow in elliptical pipe flow proved impractical (Kerswell and Davey (1996): the elliptical pipe has to have a cross-sectional aspect ratio of over 10 to become linearly unstable!). However, armed with this new approach, two groups (Faisst and Eckhardt 2003, Wedin and Kerswell 2004) have now found nonlinear travelling wave solutions in pipe flow.

To understand the mechanistic origin of these travelling waves, we decompose the 'perturbation' velocity away from HPF, that is, $\tilde{\boldsymbol{u}} := \boldsymbol{u} - (1-s^2)\hat{\boldsymbol{z}}$ into the basic building blocks of streamwise rolls, streaks and axially-dependent wave structures as follows:

$$\begin{bmatrix} \tilde{\boldsymbol{u}} \\ p \end{bmatrix} = \begin{bmatrix} U(s,\phi)\hat{\boldsymbol{s}} + V(s,\phi)\hat{\boldsymbol{\phi}} \\ P(s,\phi) \end{bmatrix}_{\text{rolls}} + \begin{bmatrix} W(s,\phi)\hat{\boldsymbol{z}} \\ 0 \end{bmatrix}_{\text{streaks}}, \tag{4.13}$$

$$+ \begin{bmatrix} \hat{\boldsymbol{u}}(s,\phi,z-ct) \\ \hat{p}(s,\phi,z-ct) \end{bmatrix}_{\text{waves}}. \tag{4.14}$$

Here c is the *a priori* unknown phase speed of the travelling wave and it is understood that the waves have no mean under streamwise averaging, that is, $\overline{\tilde{\boldsymbol{u}}}^z = \boldsymbol{U} := U\hat{\boldsymbol{s}} + V\hat{\boldsymbol{\phi}} + W\hat{\boldsymbol{z}}$ with

$$\overline{(\quad)}^z := \lim_{L\to\infty} \frac{1}{2L}\int_{-L}^{L} (\quad)\,\mathrm{d}z. \tag{4.15}$$

The governing equations (2.4) and (2.5) can be rewritten for $\tilde{\boldsymbol{u}}$ as follows.

$$\tilde{\boldsymbol{u}}_t + (1-s^2)\tilde{\boldsymbol{u}}_z - 2s\tilde{u}\hat{\boldsymbol{z}} + \tilde{\boldsymbol{u}}\cdot\boldsymbol{\nabla}\tilde{\boldsymbol{u}} + \boldsymbol{\nabla}p - \frac{1}{Re}\nabla^2\tilde{\boldsymbol{u}} = \boldsymbol{0}, \tag{4.16}$$

$$\boldsymbol{\nabla}\cdot\tilde{\boldsymbol{u}} = 0, \tag{4.17}$$

where $\tilde{\boldsymbol{u}}$ satisfies homogeneous boundary conditions and p is assumed strictly periodic in the axial direction. The equations for the streamwise rolls are $\hat{\boldsymbol{s}}\cdot\overline{(4.16)}^z$ and $\hat{\boldsymbol{\phi}}\cdot\overline{(4.16)}^z$,

$$U_t + P_s - \frac{1}{Re}\hat{\boldsymbol{s}}\cdot\nabla^2\boldsymbol{U} = -\hat{\boldsymbol{s}}\cdot(\boldsymbol{U}\cdot\boldsymbol{\nabla}\boldsymbol{U} + \overline{\hat{\boldsymbol{u}}\cdot\boldsymbol{\nabla}\hat{\boldsymbol{u}}}^z), \tag{4.18}$$

$$V_t + \frac{1}{s}P_\phi - \frac{1}{Re}\hat{\boldsymbol{\phi}}\cdot\nabla^2\boldsymbol{U} = -\hat{\boldsymbol{\phi}}\cdot(\boldsymbol{U}\cdot\boldsymbol{\nabla}\boldsymbol{U} + \overline{\hat{\boldsymbol{u}}\cdot\boldsymbol{\nabla}\hat{\boldsymbol{u}}}^z), \tag{4.19}$$

together with the incompressibility condition

$$(sU)_s + V_\phi = 0. \tag{4.20}$$

Ignoring the presence of the waves $\hat{\boldsymbol{u}}$ for the moment, small amplitude streamwise rolls will approximately satisfy the linear Stokesian problem obtained by suppressing the right-hand sides of (4.18) and (4.19). All solutions to this experience viscous decay over a timescale of $O(Re)$ and it is reasonable to take the least damped roll as a potentially typical structure for a travelling wave (see Wedin and Kerswell (2004)). For a given azimuthal wavenumber, this takes the form

$$[U, V, 0, P] := [\tilde{U}(s)\cos m\phi,\ \tilde{V}(s)\sin m\phi,\ 0,\ \tilde{P}\cos m\phi] \tag{4.21}$$

so that it is invariant under the rotational transformation

$$\mathcal{R}_m : \begin{bmatrix} u \\ v \\ w \\ p \end{bmatrix}(s,\phi,z) \to \begin{bmatrix} u \\ v \\ w \\ p \end{bmatrix}\left(s, \phi + \frac{2\pi}{m}, z\right) \tag{4.22}$$

and also invariant under the reflectional symmetry

$$\mathcal{Z} : \begin{bmatrix} u \\ v \\ w \\ p \end{bmatrix}(s,\phi,z) \to \begin{bmatrix} u \\ -v \\ w \\ p \end{bmatrix}(s,-\phi,z). \tag{4.23}$$

These rolls advect the mean shear to produce high and low-speed streaks $W(s,\phi)$ via the equation $\hat{\boldsymbol{z}}\cdot\overline{(4.16)}^z$

$$UW_s + \frac{VW_\phi}{s} - \frac{1}{Re}\nabla^2 W - 2sU = -\overline{\hat{\boldsymbol{u}}\cdot\boldsymbol{\nabla}\hat{w}}^z. \tag{4.24}$$

This is a linear inhomogeneous equation for W when the nonlinear wavelike contribution is suppressed and at a certain amplitude ϵ of the rolls, the streaks become inflexionally unstable.

Subtracting the parts of (4.16) which have been satisfied by defining the rolls and streaks leads to the wave equations

$$\hat{\boldsymbol{u}}_t + (1-s^2)\hat{\boldsymbol{u}}_z - 2s\hat{u}\hat{\boldsymbol{z}} + \boldsymbol{U}\cdot\boldsymbol{\nabla}\hat{\boldsymbol{u}} + \hat{\boldsymbol{u}}\cdot\boldsymbol{\nabla}\boldsymbol{U} + \boldsymbol{\nabla}\hat{p} - \frac{1}{Re}\nabla^2\hat{\boldsymbol{u}} = -\hat{\boldsymbol{u}}\cdot\boldsymbol{\nabla}\hat{\boldsymbol{u}} - \begin{bmatrix} \boldsymbol{U}\cdot\boldsymbol{\nabla}U - \dfrac{V^2}{s} \\ \boldsymbol{U}\cdot\boldsymbol{\nabla}V + \dfrac{UV}{s} \\ 0 \end{bmatrix}, \tag{4.25}$$

$$\boldsymbol{\nabla}\cdot\hat{\boldsymbol{u}} = 0 \tag{4.26}$$

(note this is not simply (4.16)$-\overline{(4.16)}^z$ since the roll equations solved are linearized). Dropping the right-hand side recovers the linear stability problem for the disturbance $\hat{\boldsymbol{u}}$ superimposed upon $\boldsymbol{U}$, the rolls + streaks. At marginality, a wavelike instability $\hat{\boldsymbol{u}}(\boldsymbol{x},t) = \boldsymbol{u}(s,\phi)\mathrm{e}^{\mathrm{i}\alpha(z-ct)}$ exists where c is a real frequency and α is a real wavenumber. This wavelike instability can either be symmetric or antisymmetric with respect to the shift-and-reflect symmetry

$$\mathcal{S}: \begin{bmatrix} u \\ v \\ w \\ p \end{bmatrix}(s,\phi,z) \to \begin{bmatrix} u \\ -v \\ w \\ p \end{bmatrix}\left(s,-\phi,z+\frac{\pi}{\alpha}\right), \tag{4.27}$$

that is $\mathcal{S}$-symmetric or $\mathcal{S}$-antisymmetric and can respect the symmetry $\mathcal{R}_m$ ($\mathcal{R}_m$-symmetric) or not.

At this point, the streamwise rolls are feeding energy from the mean flow into the streaks which in turn are feeding energy into the wavelike instability. For a self-sustaining cycle to be set up, the wavelike instability must inject energy back into the streamwise rolls which otherwise would secularly decay. This is ensured if the parts of the nonlinear self-interaction $\hat{\boldsymbol{u}}\cdot\boldsymbol{\nabla}\hat{\boldsymbol{u}}$ term in (4.18) and (4.19) act to force 'new' rolls of the same form as the originally chosen streamwise rolls. This positive feedback scenario has been explicitly demonstrated for an initial choice of least decaying streamwise rolls for $m = 2, 3, 4, 5$ and 6 (Wedin and Kerswell 2004). The waves can be imagined to grow in amplitude (typically reaching $O(\sqrt{\epsilon/Re})$) until their nonlinear self-interaction terms take over the role of the time derivative terms in the Stokesian operator. At this point, a steady balance exists between nonlinear wave driving and viscous diffusion of the rolls.

It is important to emphasize that this feasibility analysis includes all 'linear' aspects of the equations but ignores the majority of the nonlinear terms, specifically

$$\boldsymbol{U}\cdot\boldsymbol{\nabla}\boldsymbol{U} - (\boldsymbol{U}\cdot\boldsymbol{\nabla}W)\hat{\boldsymbol{z}} \qquad \text{and} \qquad \hat{\boldsymbol{u}}\cdot\boldsymbol{\nabla}\hat{\boldsymbol{u}} - (\hat{\boldsymbol{s}}\cdot\overline{\hat{\boldsymbol{u}}\cdot\boldsymbol{\nabla}\hat{\boldsymbol{u}}}^z)\hat{\boldsymbol{s}} - (\hat{\boldsymbol{\phi}}\cdot\overline{\hat{\boldsymbol{u}}\cdot\boldsymbol{\nabla}\hat{\boldsymbol{u}}}^z)\hat{\boldsymbol{\phi}}, \tag{4.28}$$

so the designed combination of rolls, streaks and wave represents only an approximate solution argued for in the limit of small amplitude rolls but assuming the associated streaks are large enough to be neutrally stable. To confirm the existence of a self-sustaining cycle, the full Navier–Stokes equations must be tackled.

4.1. Exact solutions via continuation

A connection can be made between the approximate feasibility analysis presented above and a more formal continuation setting by adding an artificial body force $\boldsymbol{f} := f(s,\phi)\hat{\boldsymbol{s}} + g(s,\phi)\hat{\boldsymbol{\phi}}$

to the Navier–Stokes equations which specifically targets the roll equations

$$U_t + P_s - \frac{1}{Re}\hat{\boldsymbol{s}} \cdot \nabla^2 \boldsymbol{U} + \hat{\boldsymbol{s}} \cdot (\boldsymbol{U} \cdot \boldsymbol{\nabla} \boldsymbol{U}) = f(s, \phi) - \hat{\boldsymbol{s}} \cdot (\overline{\hat{\boldsymbol{u}} \cdot \boldsymbol{\nabla} \hat{\boldsymbol{u}}}^z), \tag{4.29}$$

$$V_t + \frac{1}{s} P_\phi - \frac{1}{Re}\hat{\boldsymbol{\phi}} \cdot \nabla^2 \boldsymbol{U} + \hat{\boldsymbol{\phi}} \cdot (\boldsymbol{U} \cdot \boldsymbol{\nabla} \boldsymbol{U}) = g(s, \phi) - \hat{\boldsymbol{\phi}} \cdot (\overline{\hat{\boldsymbol{u}} \cdot \boldsymbol{\nabla} \hat{\boldsymbol{u}}}^z). \tag{4.30}$$

This body force is designed to initially maintain streamwise rolls of chosen structure against viscous decay (Faisst and Eckhardt 2003, Wedin and Kerswell 2004). The numerical procedure is then to increase $|\boldsymbol{f}|$ until the directly forced two-dimensional rolls and concomitant streak field suffers a symmetry-breaking bifurcation where a three-dimensional instability appears. Using a body force which produced the least decaying roll structure discussed above, this streak instability is found to be very similar to that predicted in the feasibility analysis (Wedin and Kerswell 2004). As a result, a streak instability which is already known to have a positive feedback onto the rolls can be pre-selected. Formally, this does not guarantee that the bifurcation is subcritical since the excitation and subsequent influence of the second harmonic is not taken into account. However, practically, ensuring positive feedback seems to invariably imply subcriticality allowing the new roll + streak + wave solution branch to be followed back to lower values of $|\boldsymbol{f}|$. In effect the two components of $\overline{\hat{\boldsymbol{u}} \cdot \boldsymbol{\nabla} \hat{\boldsymbol{u}}}^z$ start to take over the role of $\boldsymbol{f}$ in (4.29) and (4.30). Ideally, the forcing amplitude $|\boldsymbol{f}|$ can be reduced to zero at which point a fully nonlinear travelling solution to the physical pipe flow problem has been achieved.

Although the feasibility analysis is excellent in predicting which bifurcations can be tracked back, it cannot guarantee that the $|\boldsymbol{f}| = 0$ axis will ultimately be reached (before the curve bends back towards increasing $|\boldsymbol{f}|$) since this is a fully nonlinear result which can hinge on the neglected terms (4.28). A particularly stark demonstration of this is the fact that $\boldsymbol{\mathcal{S}}$-symmetric and $\boldsymbol{\mathcal{S}}$-antisymmetric wavelike instabilities can both show positive feedback onto the original rolls, but no $\boldsymbol{\mathcal{S}}$-antisymmetric waves have so far been successfully continued back to $|\boldsymbol{f}| = 0$ (Wedin (2004): the situation is apparently similar in plane Couette and Poiseuille flow too: Waleffe, private communication). The $\boldsymbol{\mathcal{S}}$-symmetric travelling waves currently known have been found only by using bifurcations where the wavelike instability shares the same $\boldsymbol{\mathcal{R}}_m$-symmetry as the underlying rolls+streaks. This has led to $\boldsymbol{\mathcal{R}}_m$-symmetric travelling waves for $m = 2, 3, 4, 5$ and 6 but not $m = 1$ (Faisst and Eckhardt 2003, Wedin and Kerswell 2004). These $\boldsymbol{\mathcal{R}}_m$ travelling waves have as their foundation a $2m$ streamwise vortex structure. Two streamwise rolls ($m = 1$) is the initial structure which experiences the most transient growth (Bergström 1993, Schmid and Henningson 1994, Zikanov 1996) but surprisingly does not seem to support a travelling wave. This emphasizes the importance of the nonlinear feedback of the streak instability onto the rolls. A $\boldsymbol{\mathcal{R}}_1$-symmetric wave can been found but only by tracking a subharmonic wavelike instability with $\boldsymbol{\mathcal{R}}_1$-symmetry upon a $\boldsymbol{\mathcal{R}}_2$-symmetric 4-roll structure (Wedin and Kerswell 2004). This has a different structure to the finite amplitude $m = 1$ wave discussed by Smith and Bodonyi (1982) in which swirl is an important component. The $\boldsymbol{\mathcal{R}}_1$-symmetric wave, along with all the other travelling waves found so far, has no swirl associated with it. Other travelling waves surely exist involving more exotic wavelike instabilities but they are more expensive to capture numerically and, if the $\boldsymbol{\mathcal{R}}_1$ wave found is any indication, probably exist at higher Re.

The travelling wave solutions currently known all appear through saddle node bifurcations at some minimum value of Re for fixed values of α over a finite range. Since ongoing pipe flow experiments (at Manchester—e.g. Hof *et al* (2003) and Delft—e.g. Hof *et al* (2004)) are constant mass flux set-ups, it makes sense to couch the results in terms of the mass-flux Reynolds number Re_m rather than the pressure gradient Reynolds number Re. The phase speed is an important *a priori* unknown feature of the waves and is a convenient coordinate against

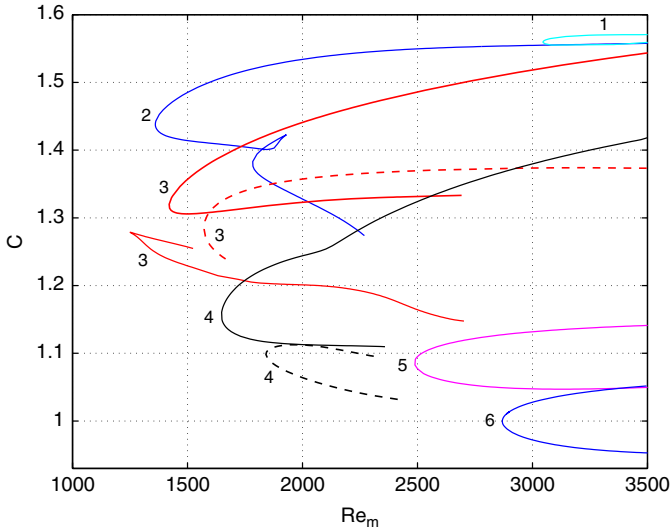

Figure 1. The phase speed normalized by the average streamwise speed, $C = c \times W/\overline{W}$ as a function of Re_m for the different m solution branches at their optimal wavenumber α^* given in table 1 (there are multiple solution branches for $m = 3$ and 4). The phase speed is seen to clearly decrease systematically with increasing m (each branch is shown only as far as it is assured to be resolved).

which to plot the wave solution surface. Figure 1 plots a single fixed α-slice through each solution surface in the three-dimensional space (Re_m, α, C) where $C = cW/\overline{W}$ is the phase speed in units of the mean axial velocity. The value of α chosen through each $\mathcal{R}_m$-symmetric solution surface corresponds to the lowest value of Re_m at the saddle node bifurcation: $\mathcal{R}_m$-symmetric solutions only exist above this. Curves are shown only as far as they prove robust against numerical truncation changes (with typically $O(16\,000)$ degrees of freedom used to represent all three velocity components and the pressure field: Wedin and Kerswell (2004)). The $\mathcal{R}_3$ and $\mathcal{R}_4$ solution surfaces are particularly interesting because there are multiple branches indicating surface folding. Table 1 collates the optimal values of α and Re which produce min Re_m as a function of m. Only travelling waves with $m = 2$, 3 and 4 exist over the normally quoted range for turbulent transition ($2000 < Re_m < 2500$). The friction factors (Schlichting (1968), equation (5.10))

$$\Lambda := \frac{1}{\rho}\frac{\mathrm{d}p}{\mathrm{d}z}\Big/\frac{1}{4s_0}\overline{W}^2 = \frac{64Re}{Re_m^2}, \tag{4.31}$$

associated with the travelling wave branches shown in figure 1 are plotted in figure 2. This shows that there are $\mathcal{R}_2$, $\mathcal{R}_3$ and $\mathcal{R}_4$ waves with dissipation rates comparable with what is observed experimentally beyond transition (e.g. at $Re_m = 2000$). The currently best (lowest) rigorous theoretical bound on the friction factor (Plasting and Kerswell 2005) is about five times higher than the experimentally observed value at $Re_m = 2000$. Interestingly however, the optimal 'velocity' field (which needs only satisfy a small subset of the dynamical constraints imposed by Navier–Stokes equations) is dominated by fast and slow streaks alternately arranged around the pipe wall. The travelling waves have a similar structure but apparently the full constraints of the Navier–Stokes equations stop them becoming so strong and close to the wall (see figure 3 of Plasting and Kerswell (2005)).

Cross-sections of all the three solutions surfaces known to exist down to $Re_m = 2000$ ($\mathcal{R}_2$, $\mathcal{R}_3$ and $\mathcal{R}_4$) are shown as a function of α in figures 3 and 4. This shows that there is also

Table 1. Optimal properties of the travelling wave solutions at their saddle node bifurcation points.

	$\mathcal{R}_1$	$\mathcal{R}_2$	$\mathcal{R}_3$	$\mathcal{R}_4$	$\mathcal{R}_5$	$\mathcal{R}_6$
$\min_\alpha Re_m$	3046	1358	1251	1647	2485	2869
Corresponding Re	3800	1663	1631	2280	3427	4069
Wavenumber α	2.17	1.55	2.44	3.23	4.11	4.73
Wavelength (in radii)	2.90	4.05	2.58	1.95	1.53	1.33
Phase velocity c	0.63	0.59	0.49	0.42	0.39	0.35
C (c in units of $\overline{W}$)	1.56	1.44	1.28	1.16	1.08	1.00
$\max \overline{\lvert w_m \rvert}^z$	0.70	0.39	0.36	0.36	0.41	0.40
$\max \overline{\lvert \tilde{u} \rvert}^z$	0.023	0.034	0.047	0.056	0.025	0.026

The value of Re corresponding to $\min Re_m$ is given although this is *not* the minimum value of this parameter only close to it. Maximum streamwise-averaged values for $w_m := \tilde{w} + (1 - Re_m/Re)(1 - s^2)$, the velocity differential of the wave above the equivalent laminar solution with the same mass flux and the radial velocity $\tilde{u}$ are given in units of $\overline{W}$ to indicate that streamwise velocities dominate transverse velocities. These figures also show that the $\mathcal{R}_1$ wave has a different character from the other waves found.

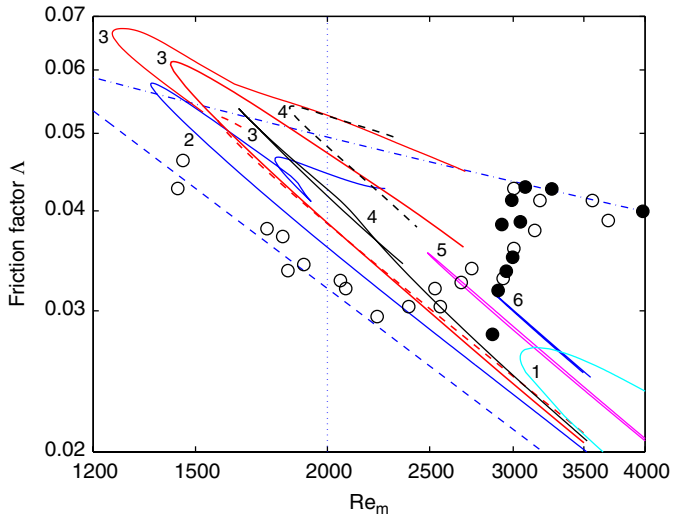

Figure 2. The friction factor $\Lambda := 64Re/Re_m^2$ for the $\mathcal{R}_m$ travelling waves branches (labelled by m) at their optimal wavenumber α^*. The straight dashed lower line represents the lower bound given by the Hagen–Poiseuille solution ($Re = Re_m$) and the upper dash–dot curve corresponds to the log-law parametrization of experimental data $1/\sqrt{\Lambda} = 2.0 \log(Re_m\sqrt{\Lambda}) - 0.8$ (see Schlichting (1968) equation (20.30)). The hollow circles are experimental data from Schlichting (1968) and the solid circles are the Oregon data from McKeon *et al* (2004b) (both indicate a slightly delayed transition past $Re_m = 2000$). The vertical dotted line at $Re_m = 2000$ indicates the slice considered in figures 3 and 4.

folding in the $\mathcal{R}_2$ surface which is missed by the optimal wavenumber slice $\alpha^* = 1.55$ shown in figure 1 (and as a vertical dashed line in figure 3). The wavelengths λ_m (in radii) of the $\mathcal{R}_m$ waves are limited to finite ranges: $3.2 \leqslant \lambda_2 \leqslant 8.0$, $2.1 \lesssim \lambda_3 \leqslant 6.1$ and $1.8 \leqslant \lambda_4 \leqslant 2.6$ at $Re_m = 2000$ with some uncertainty in the lower estimate for $\mathcal{R}_3$ due to difficulty in resolving the solution fully there (the curve becomes sensitive to the exact truncation used). The structure of the travelling waves is fairly consistent over the cross-sections (figures 5–7). There is a uniform distribution of fast streaks near the pipe wall and slow streaks in the interior. The fast streaks are very two-dimensional, hardly varying with distance down the pipe and typically

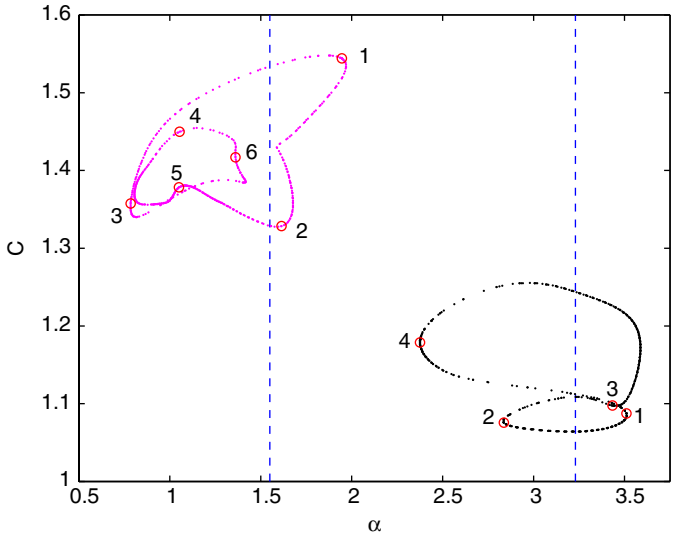

Figure 3. Cross-sections of the $\mathcal{R}_2$ and $\mathcal{R}_4$ travelling wave surfaces over α at fixed $Re_m = 2000$ (each dot represents a solution found by a branch continuation procedure). The vertical dashed lines indicate the optimal wavenumbers α^* ($\alpha_2^* = 1.55$ and $\alpha_4^* = 3.23$). The range of wavenumbers is $0.784 \leqslant \alpha \leqslant 1.97$ for $\mathcal{R}_2$ and $2.38 \leqslant \alpha \leqslant 3.59$ for $\mathcal{R}_4$. Typical solutions are labelled by numbers for referencing in following plots.

number $2m$ for $\mathcal{R}_2$, $\mathcal{R}_3$ and $\mathcal{R}_4$ waves and m for $\mathcal{R}_5$ and $\mathcal{R}_6$ waves (Wedin and Kerswell 2004). However there are exceptions, for example, solution 3 for $\mathcal{R}_3$ (see figure 4) only has m fast streaks (for more $\mathcal{R}_3$ examples see Wedin and Kerswell (2004)) and Faisst and Eckhardt (2003) discuss seeing a $2m$ fast streak $\mathcal{R}_5$ solution. Interestingly, the typically-quoted streak separation of 100 viscous wall units observed experimentally in planar shear flows translates into an angular separation of just about $2\pi/5$ around the pipe wall at $Re_m = 2000$ (taking $Re = 3100$ to be consistent with the experimental friction factor value) or five equally spaced streaks. This certainly seems to resonate with what is observed—the $\mathcal{R}_m$ wave selects m or $2m$ fast streaks depending on which is closest to 5 except for the $\mathcal{R}_4$ solution for which no m streak solution has so far been found.

The slow streaks, however, show much more three-dimensionality or variability along the pipe. Most notably, the central region around the axis can be the location of the largest negative anomaly in the travelling waves (darkest contour in figures 5–7; e.g. solution 2 in figure 6) or suffer very little adjustment when compared with the equivalent laminar state (e.g. solution 4 of figure 7). The dissipation rate associated with a travelling wave depends on the strength of the fast streaks and their proximity to the wall. Figures 8 and 9 indicate the variation in friction factor values over the $\mathcal{R}_2$, $\mathcal{R}_3$ and $\mathcal{R}_4$ cross-sections for $Re_m = 2000$. Solution 2 of the $\mathcal{R}_2$ waves, for example, has stronger streaks more tightly pressed against the wall than its neighbouring solution 1 (figure 5) and is correspondingly more dissipative.

Contour plots of the streamwise vorticity (figures 10 and 11) emphasize the staggered nature of the streamwise vortices in these travelling waves with regions of negative and positive axial vorticity wrapped around each other. This is consistent with the structure of analogous steady and travelling waves known in channel flows (Waleffe 2003). These plots taken at $Re_m = 2000$ also illustrate two other features: the wavelengths of the $\mathcal{R}_m$ waves typically shorten and the wave becomes more localized near the wall as m increases. This is also seen in figure 12 which plots the root mean square (rms) values of the azimuthal velocity and the axial

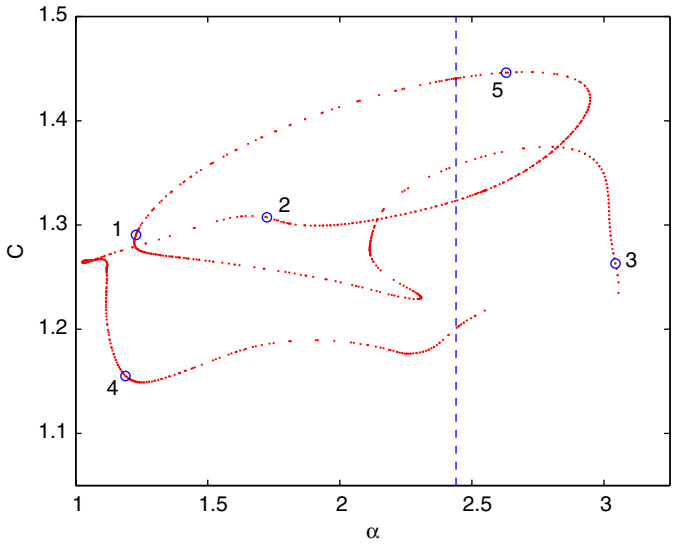

Figure 4. A cross-section of he $\mathcal{R}_3$ travelling wave surface over α at fixed $Re_m = 2000$ as far as it can be resolved using $O(16\,000)$ degrees of freedom to represent the three components of the velocity field and the pressure field. The vertical dashed line indicates the optimal wavenumber $\alpha^* = 2.44$. Solutions found have $1.03 < \alpha \lesssim 3.06$. Again, typical solutions are labelled by numbers for referencing in following plots.

velocity differential from the equivalent mass-flux laminar state ($w - Re_m/Re(1-s^2)$) for a $\mathcal{R}_2$, $\mathcal{R}_3$ and $\mathcal{R}_4$ wave at $Re_m = 2000$. The disparity in the velocity scales is also entirely typical: the streamwise (axial) velocity dominates the cross-stream (radial) and spanwise (azimuthal) velocities by an order of magnitude.

5. Significance of the travelling waves

Dynamical systems theory offers the best framework in which to understand the significance of the recently discovered travelling wave solutions. In this, pipe flow can be considered as a nonlinear dynamical system $\mathrm{d}\boldsymbol{u}/\mathrm{d}t = \boldsymbol{f}(\boldsymbol{u}; Re)$ defined by the governing Navier–Stokes equations, flow incompressibility, the appropriate pressure-gradient or constant-mass flux forcing and boundary conditions. Here $\boldsymbol{u}$ is no longer a spatially and temporally-dependent incompressible vector field but can be most conveniently considered as a large dimensional array of time-dependent scalar coefficients which arise from a Galerkin projection of the velocity field onto a complete basis of three-dimensional, incompressible spatial basis functions which each satisfy the boundary conditions. Although formally infinite dimensional, the usual argument is that the motion of a viscous fluid in a finite domain is always finite dimensional due to the viscous cutoff of fine scales (e.g. Constantin *et al* (1985) and see chapter III of Foias *et al* (2001)). The Reynolds number Re is the one parameter of the system.

As discussed above, there is one linearly-stable fixed point (HPF) for all Re which is a global attractor for $Re < Re_g$ (nonlinearly stable) but only a local attractor for $Re > Re_g$ (nonlinearly unstable but still linearly stable): experiments suggest that Re_g is around 2000. It is known that all disturbances to this basic state must decay exponentially if $Re < Re_e = 81.49$ (Joseph and Carmi 1969), the energy stability limit, whereas for $Re_e \leqslant Re < Re_g$, some disturbances can transiently grow but then decay (Boberg and Brosa 1988, Bergström 1993,

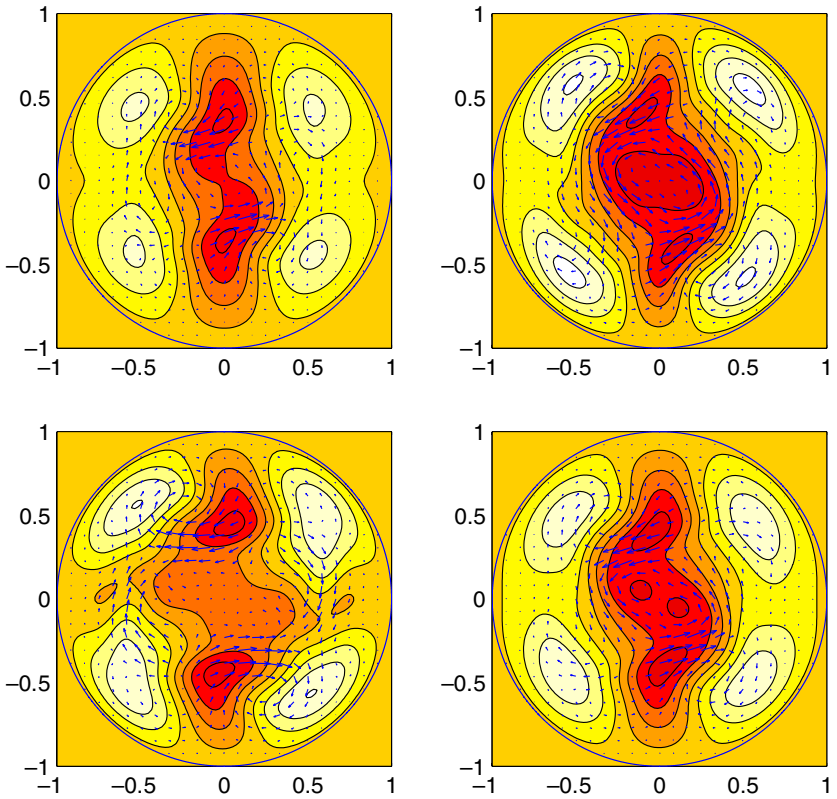

Figure 5. Typical slices across $\mathcal{R}_2$ travelling waves at $Re_m = 2000$. The arrows indicate the cross-stream velocities (larger arrows corresponding to larger speeds) and the shading represents the axial velocity differential away from the laminar flow corresponding to the same mass flux, that is, $\tilde{w} + (1 - Re_m/Re)(1 - s^2)$ (dark most negative and light most positive). The same contours are used throughout to help contrast the different solutions (the shading outside the pipe indicates 0: contours levels range from −0.37 to 0.16 in 12 steps). The lighter islands near the pipe wall indicate fast streaks whereas the darker regions near the pipe axis represent slow streaks. The solutions shown in the nomenclature of figure 3 are: 1 (upper left), 2 (upper right), 3 (lower left) and 6 (lower right) (4 looks like 6 and 5 like 3).

Schmid and Henningson 1994, O'Sullivan and Breuer 1994a, Zikanov 1996). At $Re = Re_g$, new limit sets in phase space must come into existence to prevent every trajectory ultimately spiralling down to HPF. The travelling waves found so far are all saddle points in phase space with low-dimensional unstable manifolds (Faisst and Eckhardt (2003) quote 2 unstable directions for $\mathcal{R}_2$ and 1 for $\mathcal{R}_3$ at their saddle node points and the situation is similar for $\mathcal{R}_4$, $\mathcal{R}_5$ and $\mathcal{R}_6$). These saddles presumably are organizing structures in phase space acting to attract a flow trajectory from the vicinity of the laminar state but then repelling it away and ultimately back at least for $Re \lesssim 2000$ so that the global attractor property of HPF is not disturbed. Put another way, the travelling wave solutions constitute a 'skeleton' about which complicated time-dependent orbits may drape themselves temporarily before falling back to the laminar state (this is a general idea in chaotic systems which goes back to Ruelle (1978), Eckmann and Ruelle (1985) and Cvitanović (1988) and has been suggested more recently in the context of shear flows by Schmiegel and Eckhardt (1997), Eckhardt *et al* (2002)). However as Re increases to around 2000, it is natural to speculate that the stable and unstable manifolds

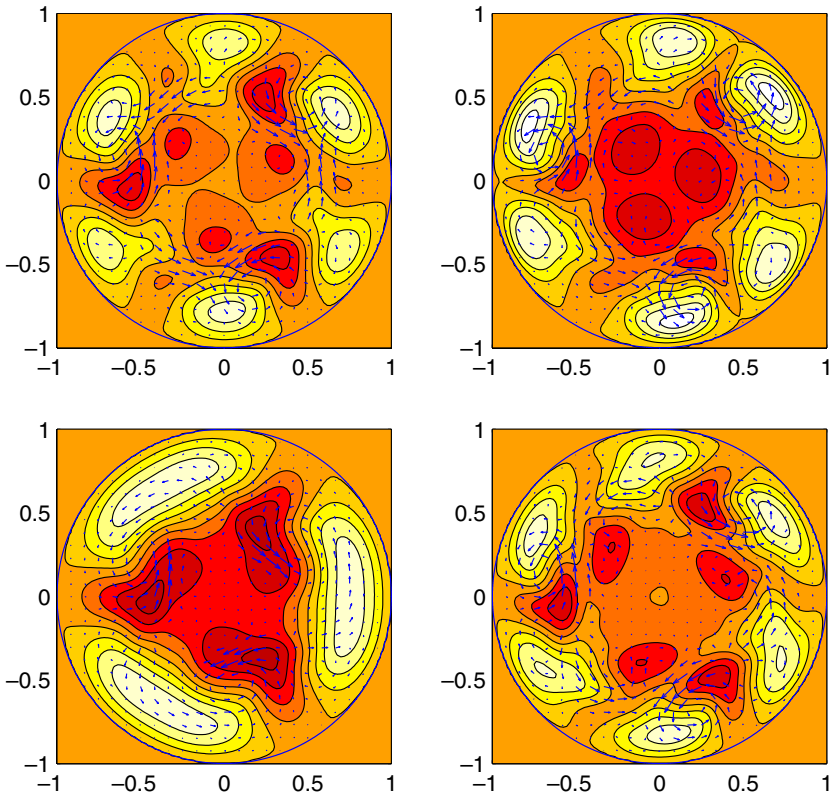

Figure 6. As in figure 5 but for $\mathcal{R}_3$ travelling waves at $Re_m = 2000$. The contours levels range from −0.29 to 0.17 in 12 steps and the solutions shown in the nomenclature of figure 4 are: 1 (upper left), 2 (upper right), 3 (lower left) and 4 (lower right) (5 looks like 1). Solution 3 has only 3-fast streaks as opposed to the other solutions and solution 2 clearly looks the most dissipative because of the large shears at the wall.

of these ever increasing number of saddle points start to connect through homoclinic and heteroclinic bifurcations, and tangle giving rise to horseshoe structures and the concomitant chaotic complexity that these imply. Moreover, one can expect other periodic orbits to be borne to further complicate phase space to the extent that at some point an attracting set emerges other than the laminar state (Kawahara and Kida (2001) have isolated two such states in plane Couette flow and Toh and Itano (2003) a periodic-like solution in plane Poiseuille flow). The fact that HPF remains a local attractor in phase space is largely secondary to the fact that its basin of attraction diminishes rapidly as *Re* increases. This, taken with the fact that the basin boundary is undoubtedly complicated in such a high dimensional phase space, explains why HPF is so sensitive to the size and form of an initial disturbance.

The appearance of a turbulent attractor is however not assured or in fact necessary to explain all experimental or numerical findings (e.g. Crutchfield and Kaneko (1988)). Pipes, whether in the laboratory or represented on the computer, are always finite and as a result long-lived transients can appear in new permanent states if they survive beyond the pipe end. In fact, Brosa (1989) has suggested that pipe flow turbulence consists *only* of transients since all initial conditions eventually relaminarized in his numerical code. In a similar vein, Faisst and Eckhardt (2004) have recently suggested that a chaotic saddle is formed at least initially in phase space for transitional *Re* following that made from similar observations in

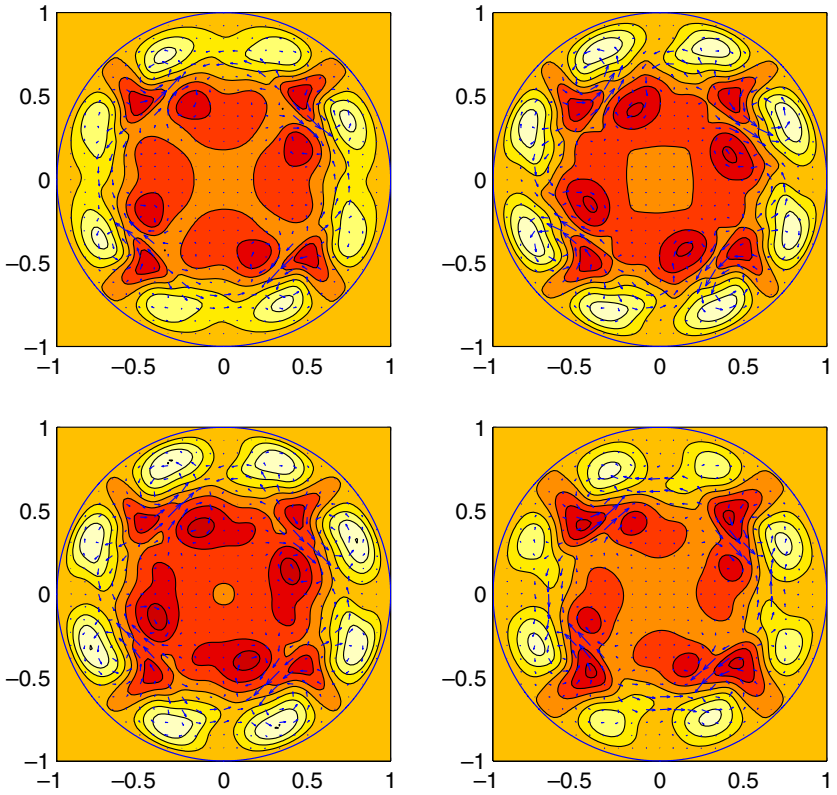

Figure 7. As in figure 5 but for $\mathcal{R}_4$ travelling waves at $Re_m = 2000$. The contours range from −0.23 to 0.15 in 12 steps and the solutions shown in the nomenclature of figure 3 are: 1 (upper left), 2 (upper right), 3 (lower left) and 4 (lower right). Due to the increased wall gradients, solutions 2 and 3 are clearly more dissipative than 1 and 4 which both have weaker fast streaks.

other shear flows (Schmiegel and Eckhardt 1997, 2000, Bottin and Chaté 1998, Bottin *et al* 1998, Faisst and Eckhardt 2000, Eckhardt *et al* 2002). Transition is then seen as an effectively statistical phenomenon in which transient lifetimes systematically increase with Re (see Mullin and Peixinho (2005) for experimental data). Once the probability of a transient surviving to the end of the pipe becomes measurable or sufficiently large—which presumably means reproducible in the laboratory—then the transitional Re is nominally reached for that pipe and environment. The characteristic features of a chaotic saddle are: a sensitive dependence of trajectory lifetimes on initial conditions (e.g. seen experimentally by Darbyshire and Mullin (1995)), an exponential distribution of lifetimes for trajectories which start 'close' to the chaotic saddle (seen experimentally by Mullin and Peixinho (2005)), positive Lyapunov exponents in the chaotic phase and independent variations of Lyapunov exponents and escape rate under changes in Re. Faisst and Eckhardt (2004) show numerical evidence for all these over the range $1600 \lesssim Re \lesssim 2250$ in a suite of calculations within a short pipe (length 10 radii) across which periodic boundary conditions are imposed. They find a lifetime divergence for $Re \approx 2250$ which they speculate could indicate the transition from a chaotic saddle to a chaotic attractor.

Some fascinating experimental evidence for the relevance of the travelling waves to transitional pipe flow has now been gathered (Hof *et al* 2004). Velocity fields measured instantaneously over a cross-sectional slice of a real transitional pipe flow show the presence

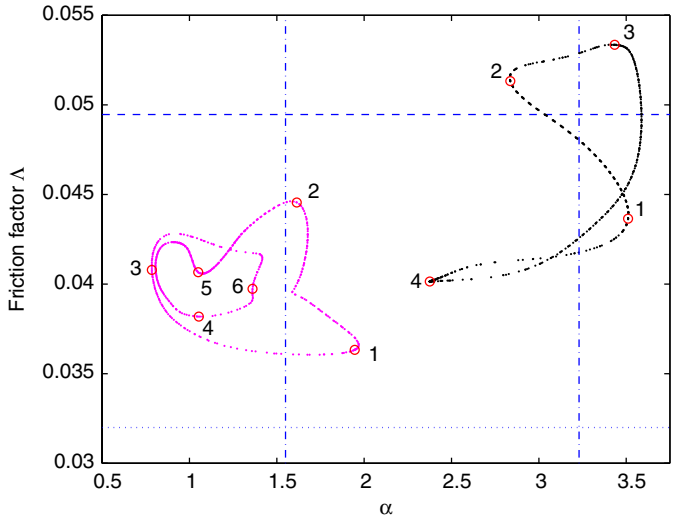

Figure 8. The friction factor $\Lambda := 64Re/Re_m^2$ for the $\mathcal{R}_2$ and $\mathcal{R}_4$ travelling wave surfaces over α at fixed $Re_m = 2000$. The vertical dashed lines indicate the optimal wavenumbers α^* ($\alpha_2^* = 1.55$ and $\alpha_4^* = 3.23$). The horizontal dotted line indicates the laminar friction factor value and the horizontal dashed line indicates the experimentally measured value at $Re = 2000$ (from the log-law parametrization). The numbers indicate the same solutions as in figure 3.

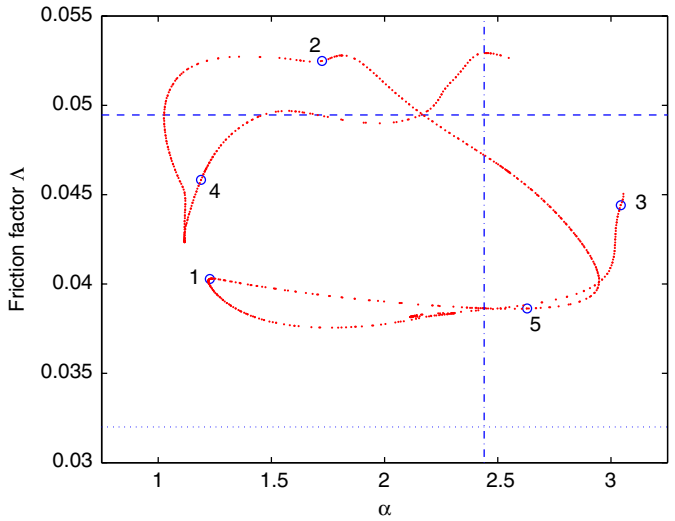

Figure 9. As in figure 8 but for $\mathcal{R}_3$ as far as can be traced. Again the numbered points correspond to the solutions already shown in figure 4.

of nearly uniformly distributed fast streaks around the pipe wall and areas of slow flow near the pipe axis in a turbulent puff. This, along with the near m-fold rotational symmetry of the experimental velocity data, resonates with the features of the $\mathcal{R}_m$-symmetric waves described above. The clear indication is that at least momentarily the flow trajectory must be getting 'close' to the travelling wave saddle point in phase space. The structural correspondence it must be said is not exact—the data seem always to have a large negative anomaly at the pipe axis

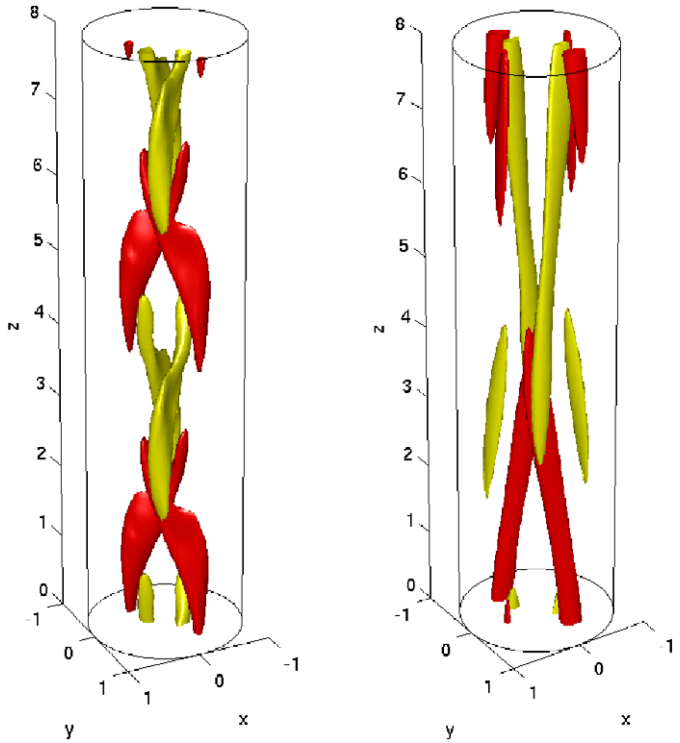

Figure 10. Isocontours of axial vorticity ω for $\mathcal{R}_2$ travelling wave solutions at $Re_m = 2000$. Two levels are shown at $\pm 60\%$ of $\max \omega$ (+ light, − dark). The solution on the left is solution 2 ($\alpha = 1.615$: two wavelengths shown) and on the right solution 3 ($\alpha = 0.785$: one wavelength shown). The interlocking of streamwise vorticity is similar to the travelling waves found in plane Poiseuille flow by Waleffe (2003, figures 15 and 16).

whereas the travelling waves do not (most notably the $\mathcal{R}_6$ wave shown in figure 2F of Hof *et al* (2004)). This can be explained away by saying that the flow trajectory will transit the vicinity of the saddle point with varying levels of approach and/or that a slightly different travelling wave is being visited (different axial wavenumber on perhaps a hitherto unknown $\mathcal{R}_m$ solution branch?). However, invoking these caveats is not entirely satisfactory and these discrepancies warrant further investigation. Hof *et al* (2004) also present some preliminary measurements of the axial coherence of $\mathcal{R}_3$- and $\mathcal{R}_4$-looking velocity fields in a puff. Interestingly, they find a 3-fast streak structure over four pipe diameters followed by what looks to be a 6-fast streak structure over the next two pipe diameters at $Re_m = 2000$: figure 6 indicates that 3-streak and 6-streak $\mathcal{R}_3$ travelling wave solutions co-exist at this Re_m.

Detailed quantitative comparisons with experimental or DNS data have yet to be carried out however. In plane Couette and Poiseuille flow, structural comparisons have been made between the mean and streamwise-fluctuating velocity components of the travelling waves known there and the statistics of turbulent flows (Jimenéz and Simens 2001, Waleffe 2003). Even though the travelling waves are strictly ordered in space and time, there is encouraging correspondence both in the spatial (streamwise and spanwise) scales and the rms values of the various velocity components. Jimenéz *et al* (2005) have recently gone further to show that near-wall turbulence stays 'close' to the upper branch travelling wave solutions in between extreme short-lived visits to other parts of phase space (see also Toh and Itano (2005)). In severely

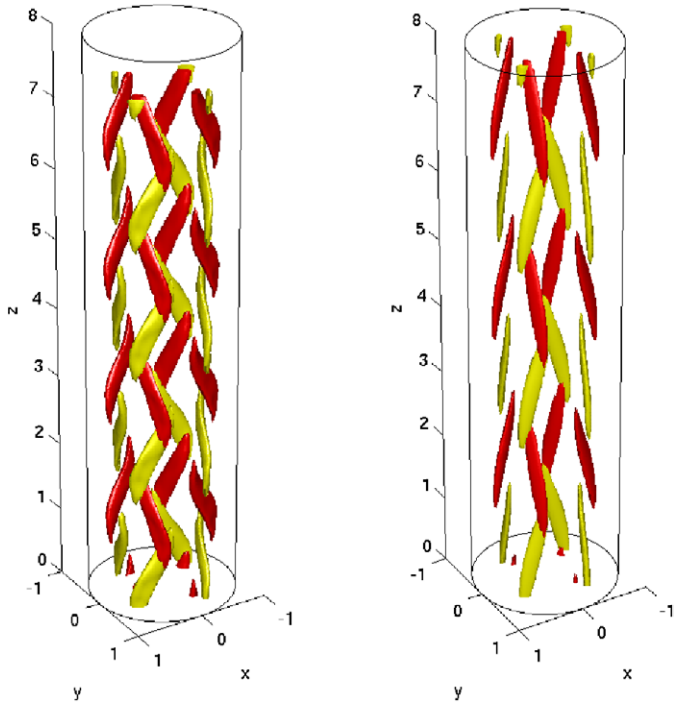

Figure 11. Isocontours of axial vorticity ω for $\mathcal{R}_4$ travelling wave solutions at $Re_m = 2000$. Two levels are shown at $\pm 60\%$ of max ω (+ light, − dark). The solution on the left is solution 3 ($\alpha = 3.434$: four wavelengths shown) and on the right solution 4 ($\alpha = 2.376$: three wavelengths shown). The axial scale is purposely the same as figure 10 to aid comparison.

confined geometries at low *Re*, these transient excursions can be towards the lower branches of travelling wave solutions (Kawahara and Kida 2001) but this is not so clear at higher *Re* or less-constrained flows (Jimenéz *et al* 2005). Current thinking, plausibly enough, views the lower branch travelling wave solutions and their stable manifolds as acting as a separatrix between the basin of attraction of the laminar state and the turbulent domain in phase space (Itano and Toh 2001, Toh and Itano 2001, Waleffe 2003).

6. Outlook

It should be clear that there are many challenges for the future. Perhaps the first is to confirm the dynamic importance of the travelling waves in transitional flows. At present, experimental evidence for their physical relevance is emerging but cannot be yet considered unequivocal. Furthermore, the signatures of these travelling waves have yet to be reported within DNS data sets although the search has admittedly only just started. Above and beyond this issue, there is the question of whether these travelling waves actively structure the flow trajectory in phase space or are just passive secondary objects visited only occasionally by the flow. The low-dimensionality of their unstable manifolds would suggest the former 'active' scenario where the flow trajectory is imagined as 'pinging' between the travelling waves in phase space like a ball in a pinball machine. Assuming that the time transiting between the (phase space) neighbourhoods of the waves is small compared to the time actually spent in these, the averaged properties of a transitional flow may be well represented by a time-weighted sum of

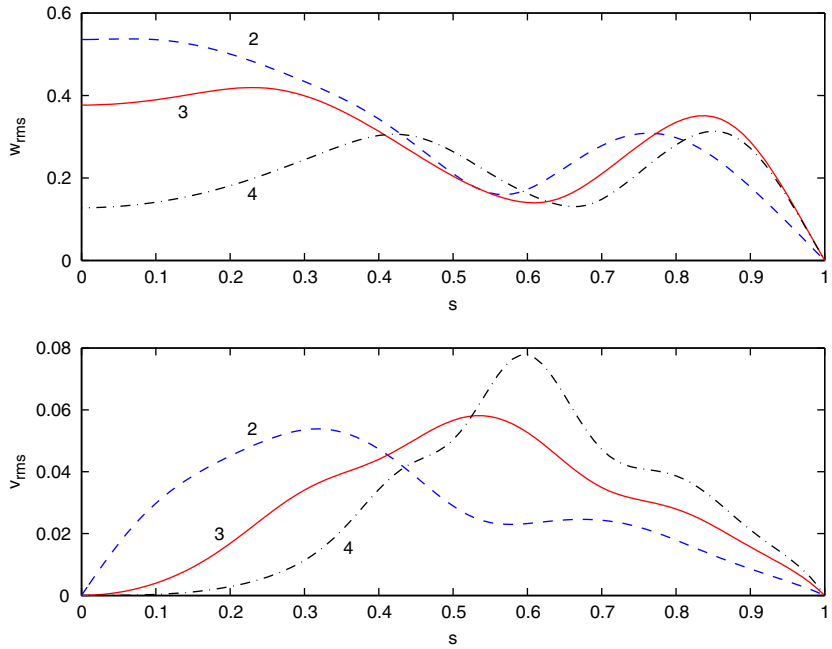

Figure 12. Rms velocities (labelled by m value) for typical $\mathcal{R}_2$, $\mathcal{R}_3$ and $\mathcal{R}_4$ waves at $Re_m = 2000$ plotted over the radius s. The most dissipative wave is chosen for each (solution 2 for $\mathcal{R}_2$ and $\mathcal{R}_3$, and solution 3 for $\mathcal{R}_4$: see figures 8 and 9). $v_{\rm rms}(s) := \sqrt{\alpha/(2\pi)^2 \int_0^{2\pi/\alpha}\int_0^{2\pi} |\tilde{v}|^2 \,{\rm d}z\,{\rm d}\phi}$ and $w_{\rm rms}(s) := \sqrt{\alpha/(2\pi)^2 \int_0^{2\pi/\alpha}\int_0^{2\pi} |w - Re_m/Re(1-s^2)|^2 \,{\rm d}z\,{\rm d}\phi}$ so that $w_{\rm rms}$ is the rms of the axial velocity differential away from the equivalent mass-flux laminar state. All velocities are shown in units of the mean axial velocity of the flow $\overline{W}$. It is clear that as m increases both the fast and slow streaks move outwards towards the pipe wall. Note also the disparity in the magnitudes of the streamwise and cross-stream velocities in these waves (the radial velocity is the same order as the azimuthal velocity component).

the properties associated with the dynamically important travelling wave solutions. Adding the contributions from the next in the hierarchy of unstable periodic solutions could improve matters further (Cvitanović 1988). This is certainly an appealing picture but is of course only speculation in the absence of solid evidence. Support for such a situation is, however, starting to emerge in plane Couette and plane Poiseuille flow as discussed above.

The gap between the first appearance of travelling wave solutions at $Re_m = 1251$ and the commonly quoted transitional value of $Re_m \approx 2000$ suggests that simply the presence of the travelling waves is far from the whole story. There appears no significant change in the structure of the waves as Re_m increases through the range $Re_m = 1750$–2300 for example, and this probably extends to their local stability properties too. Undoubtedly, what does change is the global connections between the stable and unstable manifolds of the various travelling waves. It is also hard not to imagine other (unstable) periodic orbits being borne in the meantime and contributing to the phase space complexity which is necessary to sustain the seemingly 'disordered' flow dynamics seen at transition. Verifying these ideas, however, is a formidable task probably best pursued in more accessible planar shear flows like plane Couette and plane Poiseuille flow where similar gaps exist. In plane Couette flow, steady solutions have been found down to $Re = 125$ (Nagata (1990), or more accurately 127.7 Waleffe (2003)) whereas transition is seen at $Re \approx 320$–350 (Lundbladh and Johansson 1991,

Tillmark and Alfredsson 1992, Daviaud *et al* 1992, Dauchot and Daviaud 1995, Bottin *et al* 1998) and travelling waves in plane Poiseuille flow occur down to $Re = 997$ (Waleffe 2003) compared to transition at $Re \approx 2100$–2300 (Rozhdestvensky and Simakin 1984, Keefe *et al* 1992).

Understanding how large and in what form disturbances need to be to trigger flow transition permanently is a continuing challenge. This requires characterizing the boundary of the basin of attraction of HPF which, given the high-dimensionality of transitional flow dynamics, seems inevitably a complicated multi-dimensional object. Uncertainty in setting up initial conditions near this in an experiment would explain the apparent stochasticity associated with transition observed in the laboratory. Whether knowledge of the travelling waves 'nearest' to HPF in phase space and their stable manifolds can help remains to be seen. It may, in fact, be better to try to understand the process of relaminarization (as *Re* decreases) instead, which is probably a more robust and reproducible phenomenon than transition (as *Re* increases). This change of approach has certainly paid dividends in DNS studies and seems ripe for exploitation in the laboratory.

Finally, given that the most frequently quoted practical reason for studying transition to turbulence is to try to delay or even prevent it, can the discovery of travelling waves in pipe flow help? Implicit in much of the above discussion is the thinking that the emergence of the travelling waves is a necessary precursor (as *Re* increases) to transition. This suggests concentrating on delaying their emergence or ideally eliminating them completely to control the flow. This is perhaps the most daunting of all the outstanding challenges outlined above.

Acknowledgments

The author is very grateful to Bruno Eckhardt, Tom Mullin and Fabian Waleffe for providing valuable comments on earlier drafts of this paper.

References

Artuso R, Aurell E and Cvitanovic P 1990a Recycling of strange sets: I. cycle expansions *Nonlinearity* **3** 325

Artuso R, Aurell E and Cvitanovic P 1990b Recycling of strange sets: II. applications *Nonlinearity* **3** 361

Baggett J S and Trefethen L N 1997 Low-dimensional models of subcritical transition to turbulence *Phys. Fluids* **9** 1043

Barenghi C F 2004 Turbulent transition for fluids *Phys. World* **17** 17

Barnes D R and Kerswell R R 2000 New results in rotating Hagen–Poiseuille flow *J. Fluid Mech.* **417** 103

Benney D J 1961 A non-linear theory of oscillations in a parallel flow *J. Fluid Mech.* **10** 209

Benney D J 1964 Finite amplitude effects in an unstable laminar boundary layer *Phys. Fluids* **7** 319

Benney D J and Bergeron R F 1969 A new class of nonlinear waves in parallel flows *Stud. Appl. Math.* **48** 181

Benney D J and Gustavsson L H 1981 A new mechanism for linear and nonlinear hydrodynamic instability *Stud. Appl. Math.* **64** 185

Bergström L 1992 Initial algebraic of small disturbances in pipe Poiseuille flow *Stud. Appl. Math.* **87** 61

Bergström L 1993 Optimal growth of small disturbances in pipe Poiseuille flow *Phys. Fluids* **5** 2710

Binnie A M and Fowler J S 1947 A study by a double refraction method of the development of turbulence in a long cylindrical tube *Proc. R. Soc. Lond.* A **192** 32

Blasius P R H 1913 Das Ähnlichkeitsgestz bei Reibungsvorgängen in Flüssigkeiten *Forsch. Arb. Ing.-Wes.* **131**

Boberg L and Brosa U 1988 Onset of turbulence in a pipe *Z. Naturforsch* **43** 697

Bottin S and Chaté H 1998 Statistical analysis of the transition to turbulence in plane Couette flow *Eur. Phys. J.* B **6** 143

Bottin S, Dauchot O, Daviaud F and Manneville P 1998 Experimental evidence of streamwise vortices as finite amplitude solutions in transitional plane Couette flow *Phys. Fluids* **10** 2597

Brosa U 1989 Turbulence without strange attractor *J. Stat. Phys.* **55** 1303

Brosa U and Grossmann S 1999 Minimum description of the onset of pipe turbulence *Eur. Phys. J.* B **9** 343

Butler K M and Farrell B F 1993 Optimal perturbations and streak spacing in wall-bounded shear flows *Phys. Fluids* **5** 774
Busse F H 2004 Visualising the dynamics of the onset of turbulence *Science* **305** 1574
Case K M 1960 Stability of inviscid plane Couette flow *Phys. Fluids* **3** 143
Christiansen F, Cvitanovic P and Putkaradze V 1997 Hopf's last hope: spatiotemporal chaos in terms of unstable recurrent patterns *Nonlinearity* **10** 50
Clever R M and Busse F H 1992 Three-dimensional convection in a horizontal fluid layer subjected to a constant shear *J. Fluid Mech.* **234** 511
Clever R M and Busse F H 1997 Tertiary and quaternary solutions for plane Couette flow *J. Fluid Mech.* **344** 137
Constantin P, Foias C, Manley O P and Teman R 1985 Determining modes and fractal dimension of turbulent flows *J. Fluid Mech.* **150** 427
Crutchfield J P and Kaneko K 1988 Are attractors relevant to turbulence? *Phys. Rev. Lett.* **60** 2715
Cvitanović P 1988 Invariant measurement of strange sets in terms of cycles *Phys. Rev. Lett.* **61** 2729
Cvitanović P 1992 Periodic orbit theory in classical and quantum mechanics *Chaos* **2** 1
Cvitanović P, Artuso R, Dahlqvist P, Mainieri R, Tanner G, Vattay G, Whelan N and Wirzba A 2005 *Classical and Quantum Chaos* webbook available at http://chaosbook.org
Darbyshire A G and Mullin T 1995 Transition to turbulence in constant-mass-flux pipe flow *J. Fluid Mech.* **289** 83
Dauchot O and Daviaud F 1995 Finite amplitude perturbation and spots growth mechanism in plane Couette flow *Phys. Fluids* **7** 335
Dauchot O and Vioujard N 2000 Phase space analysis of a dynamical model for the subcritical transition to turbulence in plane Couette flow *Eur. Phys. J.* B **14** 377
Davey A and Drazin P G 1969 The stability of Poiseuille flow in a pipe *J. Fluid Mech.* **36** 209
Davey A and Nguyen H P F 1971 Finite-amplitude stability of pipe flow *J. Fluid Mech.* **45** 701
Davey A 1978 On Itoh's finite amplitude stability theory for pipe flow *J. Fluid Mech.* **86** 695
Daviaud F, Hesketh J and Bergé P 1992 Subcritical transition to turbulence in plane Couette flow *Phys. Rev. Lett.* **69** 2511
Draad A A, Kuiken G D C and Nieuwstadt F T M 1998 Laminar-turbulent transition in pipe flow for Newtonian and non-Newtonian fluids *J. Fluid Mech.* **377** 267
Eckmann J-P and Ruelle D 1985 Ergodic-theory of chaos and strange attractors *Rev. Mod. Phys.* **57** 617
Eckhardt B, Faisst H, Schmiegel A and Schumacher J 2002 Turbulence transition in shear flows *Advances in Turbulence IX: Proc. 9th European Turbulence Conf. (Southampton)* ed I P Castro *et al* (Barcelona: CISME) p 701
Eckhardt B and Pandit R 2003 Noise correlations in shear flows *Eur. Phys. J.* B **33** 373
Eggels J G M, Unger F, Weiss M H, Westerweel J, Adrian R J, Friedrich R and Nieuwstadt F T M 1994 Fully developed turbulent pipe flow: a comparison between direct numerical simulation and experiment *J. Fluid Mech.* **268** 175
Eliahou S, Tumin A and Wygnanski I 1998 Laminar-turbulent transition in Poiseuille pipe flow subjected to periodic perturbation emanating from the wall *J. Fluid Mech.* **361** 333
Faisst H and Eckhardt B 2000 Transition from the Couette–Taylor system to the plane Couette system *Phys. Rev.* E **61** 7227
Faisst H and Eckhardt B 2003 Travelling waves in pipe flow *Phys. Rev. Lett.* **91** 22
Faisst H and Eckhardt B 2004 Sensitive dependence on initial conditions in transition to turbulence in pipe flow *J. Fluid Mech.* **504** 343
Fitzgerald R 2004 New experiments set the scale for the onset of turbulence in pipe flow *Phys. Today* **57** 21
Foias O, Manley O, Rosa R and Teman R 2001 *Navier–Stokes Equations and Turbulence* (Cambridge: Cambridge University Press)
Fox J A, Lessen M and Bhat W V 1968 Experimental investigation of the stability of Hagen–Poiseuille flow *Phys. Fluids* **11** 1
Garg V K and Rouleau WT 1972 Linear stability of pipe Poiseuille flow *J. Fluid Mech.* **54** 113
Gavarini M I, Bottaro A and Nieuwstadt F T M 2004 The initial stage of transition in pipe flow: role of optimal base-flow distortions *J. Fluid Mech.* **517** 131
Gebhardt T and Grossman S 1994 Chaos transition despite linear stability *Phys. Rev.* E **50** 3705
Gill A E 1965 On the behaviour of small disturbances to Poiseuille flow in a circular pipe *J. Fluid Mech.* **21** 145
Gill A E 1973 The least damped disturbance to Poiseuille flow in a circular pipe *J. Fluid Mech.* **61** 97
Grossman S 2000 The onset of shear flow turbulence *Rev. Mod. Phys.* **72** 603
Gustavsson L H 1991 Energy growth of three-dimensional disturbances in plane Poiseuille flow *J. Fluid Mech.* **224** 241
Hagen G H L 1839 Über die Bewegung des Wassers in engen cylindrischen Röhren *Poggendorfs Annalen der Physik und Chemie* **16** 423
Hamilton J M, Kim J and Waleffe F 1995 Regeneration mechanisms of near-wall turbulence structures *J. Fluid Mech.* **287** 317

Han G, Tumin A and Wygnanski I 2000 Laminar-turbulent transition in Poiseuille pipe flow subjected to periodic perturbation emanating from the wall. Part 2. Late stage of transition *J. Fluid Mech.* **419** 1

Herron I 1991 Observations on the role of vorticity in the stability theory of wall bounded flows *Stud. Appl. Math.* **85** 269

Hof B, Juel A and Mullin T 2003 Scaling of the turbulence transition threshold in a pipe *Phys. Rev. Lett.* **91** 244502

Hof B, van Doorne C W H, Westerweel J, Nieuwstadt F T M, Faisst H, Eckhardt B, Wedin H, Kerswell R R and Waleffe F 2004 Experimental observation of nonlinear travelling waves in turbulent pipe flow *Science* **305** 1594

Itano T and Toh S 2001 The dynamics of bursting process in wall turbulence *J. Phys. Soc. Japan* **70** 701

Itoh N 1977 Nonlinear stability of parallel flows with subcritical Reynolds numbers. Part 2. Stability of pipe Poiseuille flow to finite axisymmetric disturbances *J. Fluid Mech.* **82** 469

Jimenéz J and Moin P 1991 The minimal flow unit in near-wall turbulence *J. Fluid Mech.* **225** 213

Jimenéz J and Simens M P 2001 Low-dimensional dynamics in a turbulent wall flow *J. Fluid Mech.* **435** 81

Jimenéz J, Kawahara G, Simens M P and Nagata M 2005 Characterization of near-wall turbulence in terms of equilibrium and 'bursting' solutions *Phys. Fluids* **17** 015105-1

Joseph D D and Carmi S 1969 Stability of Poiseuille flow in pipes, annuli and channels *Q. Appl. Math.* **26** 575

Kawahara, G and Kida S 2001 Periodic motion embedded in plane Couette turbulence: regeneration cycle and burst *J. Fluid Mech.* **449** 291

Keefe L, Moin P and Kim J 1992 The dimension of attractors underlying periodic turbulent Poiseuille flow *J. Fluid Mech.* **242** 1

Lord Kelvin 1887a Stability of fluid motion—rectilinear motion of viscous fluid between two parallel plates *Phil. Mag.* **24** 188

Lord Kelvin 1887b Stability of motion—broad river flowing down an inclined plane bed *Phil. Mag.* **24** 272

Kerswell R R and Davey A 1996 On the linear instability of elliptic pipe flow *J. Fluid Mech.* **316** 307

Landman M J 1990 On the generation of helical waves in circular pipe flow *Phys. Fluids* **2** 738

Leite R J 1959 An experimental investigation of the stability of Poiseuille flow *J. Fluid Mech.* **5** 81

Leonard A and Reynolds W C 1985 Turbulence research by numerical simulation *Proc. Symp. held on the occasion of the 70th birthday of Hans Wolfgang Liepmann* (*Lecture Notes in Physics* vol 320) ed D Coles (Berlin: Springer) p 113

Lessen M, Sadler G S and Liu T-Y 1968 Stability of pipe Poiseuille flow *Phys. Fluids* **11** 1404

Lindgren E R 1958 The transition process and other phenomena in viscous flow *Arkiv für Physik* **12** 1

Lundbladh A and Johansson A V 1991 Direct simulation of turbulent spots in plane Couette flow *J. Fluid Mech.* **229** 499

Ma B, van Doorne C W H, Zhang Z and Nieuwstadt F T M 1999 On the spatial evolution of a wall-imposed periodic disturbance in pipe Poiseuille flow at $Re = 3000$. Part 1. Subcritical disturbance *J. Fluid Mech.* **398** 181

Mackrodt P-A 1976 Stability of Hagen–Poiseuille flow with superimposed rigid rotation *J. Fluid Mech.* **103** 241

Mariotte E 1686 Traité du mouvement des eaux et les autres corps fluides *Paris*

McKeon B J, Li J, Jiang W, Morrison J F and Smits A J 2004a Further observations on the mean velocity distribution in fully developed pipe flow *J. Fluid Mech.* **501** 135

McKeon B J, Swanson C J, Zagarola M V, Donnelly R J and Smits A J 2004b Friction factors for smooth pipe flow *J. Fluid Mech.* **511** 41

Meseguer A and Trefethen L N 2003 Linearized pipe flow to Reynolds number 10^7 *J. Comput. Phys.* **186** 178

Moehlis J, Faisst H and Eckhardt B 2004 A low-dimensional model for turbulent shear flows *New J. Phys.* **6** 56

Moehlis J, Faisst H and Eckhardt B 2005 Periodic orbits and chaotic sets in a low-dimensional model for shear flows *SIAM J. Appl. Dyn. Syst.* **4** 352

Mullin T 2005 Experimental investigations of the transition to turbulence in a circular pipe *Proc. R. Soc. Lond.* in preparation

Mullin T and Peixinho J 2005 Recent observations in the transition to turbulence in a pipe *Proc. IUTAM Bangalore Workshop on Transition* at press

Nagata M 1990 Three-dimensional finite-amplitude solutions in plane Couette flow: bifurcation from infinity *J. Fluid Mech.* **217** 519

Nagata M 1997 Three-dimensional traveling-wave solutions in plane Couette flow *Phys. Rev.* E **55** 2023

Nagata M 1998 Tertiary solutions and their stability in rotating plane Couette flow *J. Fluid Mech.* **358** 357

Nikitin N V 1994 Direct numerical modeling of three-dimensional turbulent flows in pipes of circular cross section *Fluid Dyn.* **29** 749

Nikuradse J 1932 Gesetzmässigkeit der turbulenten Strömung in glatten Röhren *Forsch. Arb. Ing.-Wes.* **356**

O'Sullivan P L and Breuer K S 1994a Transient growth in circular pipe flow. I. Linear disturbances *Phys. Fluids* **6** 3643

O'Sullivan P L and Breuer K S 1994b Transient growth in a circular pipe flow. II. Nonlinear development *Phys. Fluids* **6** 3652

Orszag S A and Patera A T 1983 Secondary instability of wall-bounded shear flows *J. Fluid Mech.* **128** 347
Patera A T and Orszag S A 1981 Finite-amplitude stability of axisymmetric pipe flow *J. Fluid Mech.* **112** 467
Pfenniger W 1961 Transition in the inlet length of tubes at high Reynolds numbers *Boundary Layer and Flow Control* ed G V Lachman (Oxford: Pergamon) p 970
Plasting S C and Kerswell R R 2005 A friction factor bound for transitional pipe flow *Phys. Fluids* **17** 011706-1
Poiseuille J L M 1840 Recherches expérimentelles sur le mouvement des liquides dans les tubes de très petits diamètres *C. R. Acad. Sci.* **11** 961
Poiseuille J L M 1840 Recherches expérimentelles sur le mouvement des liquides dans les tubes de très petits diamètres *C. R. Acad. Sci.* **11** 1041
Poiseuille J L M 1841 Recherches expérimentelles sur le mouvement des liquides dans les tubes de très petits diamètres *C. R. Acad. Sci. Paris* **12** 112–5
Prandtl L 1927 Über den Reibungswiderstand strömender Luft *Ergebnisse AVA Göttingen* **3** 1–5
Priymak V G and Miyazaki T 1998 Accurate Navier–Stokes investigation of transitional and turbulent flows in a circular pipe *J. Comput. Phys.* **142** 370
Priymak V G and Miyazaki T 2004 Direct numerical simulation of equilibrium spatially localized structures in pipe flow *Phys. Fluids* **16** 4221
Lord Rayleigh 1892 On the question of stability of the flow of fluids *Phil. Mag.* **34** 59
Reddy S C and Hennyson D S 1993 Energy growth in viscous channel flows *J. Fluid Mech.* **252** 209
Reddy S C, Schmid P J, Baggett J S and Henningson D S 1998 On stability of streamwise streaks and transition thresholds in plane channel flows *J. Fluid Mech.* **365** 269
Reshotko E and Tumin A 1999 Spatial theory of transient growth in a circular pipe flow *Bull. Am. Phys. Soc.* **44** 72
Reuter J and Rempfer D 2004 Analysis of pipe flow transition. Part 1. Direct numerical simulation *Theor. Comput. Fluid Dyn.* **17** 273
Reynolds O 1883 An experimental investigation of the circumstances which determine whether the motion of water shall be direct or sinuous, and of the law of resistance in parallel channels *Proc. R. Soc. Lond.* **35** 84
Rouse H and Ince S 1957 *History of Hydraulics* Iowa Institute of Hydraulic Research
Rozhdestvensky B L and Simakin I N 1984 Secondary flows in a plane channel: their relationship and comparison with turbulent flows *J. Fluid Mech.* **147** 261
Rubin Y, Wygnanski I J and Haritonidis J H 1980 Further observations on transition in a pipe *Proc. IUTAM Symp. on Laminar-Turbulent Transition (Stuttgart, FRG 1979)* ed R Eppler and F Hussein (Berlin: Springer) pp 19–26
Ruelle D 1978 *Statistical Mechanics, Thermodynamics Formalism* (Reading, MA: Addison-Wesley)
Salwen H and Grosch C E 1972 The stability of Poiseuille flow in a pipe of circular cross-section *J. Fluid Mech.* **54** 93
Salwen H, Cotten F W and Grosch C E 1980 Linear stability of Poiseuille flow in a circular pipe *J. Fluid Mech.* **98** 273
Schlichting H 1968 *Boundary-Layer Theory* (New York: McGraw-Hill)
Schmid P J and Henningson D S 1994 Optimal energy density growth in Hagen–Poiseuille flow *J. Fluid Mech.* **277** 197
Schmiegel A and Eckhardt E 1997 Fractal stability border in plane Couette flow *Phys. Rev. Lett.* **79** 5250
Schmiegel A and Eckhardt E 2000 Persistent turbulence in annealed plane Couette flow *Europhys. Lett.* **51** 395
Sexl T 1927 Zur stabilitatsfrage der Poiseuilleschen und Couetteschen stromung *Ann. Phys., Lpz.* **83** 835
Shan H, Ma B, Zhang Z and Nieuwstadt F T M 1999 Direct numerical simulation of a puff and a slug in transitional cylindrical pipe flow *J. Fluid Mech.* **387** 39
Smith F T and Bodonyi R J 1982 Amplitude-dependent neutral modes in the Hagen–Poiseuille flow through a circular pipe *Proc. R. Soc. Lond.* A **384** 463
Stuart J T 1965 The production of intense shear layers by vortex stretching and convection *NATO AGARD Report* No 514 1
Sutera S P and Skalak R 1993 The history of Poiseuille's law *Ann. Rev. Fluid Mech.* **25** 1
Swanson C J, Julian B, Ihas G G and Donnelly R J 2002 Pipe flow measurements over a wide range of Reynolds numbers using liquid helium and various gases *J. Fluid Mech.* **461** 51
Tillmark N and Alfredsson P H 1992 Experiments on transition in plane Couette flow *J. Fluid Mech.* **235** 89
Toh S and Itano T 2001 On the regeneration mechanism of turbulence in channel flow *Proc. IUTAM Symp. on Geometry and Statistics of Turbulence* ed T Kambe *et al* (Dordrecht: Kluwer) p 305
Toh S and Itano T 2003 A periodic-like solution in channel flow *J. Fluid Mech.* **481** 67
Toh S and Itano T 2005 Interaction between a large-scale structure and near-wall structures in channel flow *J. Fluid Mech.* **524** 249
Toplosky N and Akylas T R 1988 Nonlinear spiral waves in rotating pipe flow *J. Fluid Mech.* **190** 39
Trefethen L N, Trefethen A E, Reddy S C and Driscoll T A 1993 Hydrodynamic stability without eigenvalues *Science* **261** 578
Tumin A 1996 Receptivity of pipe Poiseuille flow *J. Fluid Mech.* **315** 119

Waleffe F, Kim J and Hamilton J 1993 On the origin of streaks in turbulent shear flows *Turbulent Shear Flows 8: Selected Papers from the 8th Int. Symp. on Turbulent Shear Flows (Munich, 9–11 September 1991)* ed F Durst *et al* (Berlin: Springer) pp 37–49

Waleffe F 1995a Transition in shear flows: nonlinear normality versus non-normal linearity *Phys. Fluids* **7** 3060

Waleffe F 1995b Hydrodynamic stability and turbulence: beyond transients to a self-sustaining process *Stud. Appl. Math.* **95** 319

Waleffe F 1997 On a self-sustaining process in shear flows *Phys. Fluids* **9** 883

Waleffe F 1998 Three-dimensional coherent states in plane shear flows *Phys. Rev. Lett.* **81** 4140

Waleffe F 2001 Exact coherent structures in channel flow *J. Fluid Mech.* **435** 93

Waleffe F 2003 Homotopy of exact coherent structures in plane shear flows *Phys. Fluids* **15** 1517–34

Waleffe F 2004 Private communication

Walton A G 2002 The temporal evolution of neutral modes in impulsively started flow through a circular pipe and their connection to the nonlinear stability of Hagen–Poiseuille flow *J. Fluid Mech.* **457** 339

Wedin H 2004 Nonlinear solutions to pipe flow *PhD Thesis* University of Bristol

Wedin H and Kerswell R R 2004 Exact coherent structures in pipe flow: travelling wave solutions *J. Fluid Mech.* **508** 333

Wygnanski I J and Champagne F H 1973 On transition in a pipe. Part 1. The origin of puffs and slugs and the flow in a turbulent slug *J. Fluid Mech.* **59** 281

Wygnanski I J, Sokolov M and Friedman D 1975 On transition in a pipe. Part 2. The equilibrium puff *J. Fluid Mech.* **69** 283

Zagarola M V and Smits A J 1998 Mean-flow scaling of turbulent pipe flow *J. Fluid Mech.* **373** 33

Zikanov O Y 1996 On the instability of pipe Poiseuille flow *Phys. Fluids* **8** 2923